Time-Domain Synthesis of Continuous-Time Filters using Nonlinear Sequence Transformation

THESIS

Submitted in partial fulfilment
of the requirements for the degree of
DOCTOR OF PHILOSOPHY

by

Goutham Makkena
ID. No. 2009PH230002H

Under the Supervision of
Dr. M. B. Srinivas

BITS Pilani
Pilani | Dubai | Goa | Hyderabad

BIRLA INSTITUTE OF TECHNOLOGY AND SCIENCE - PILANI
2017

BIRLA INSTITUTE OF TECHNOLOGY AND SCIENCE - PILANI

CERTIFICATE

This is to certify that the thesis entitled, "Time -Domain Synthesis of Continuous-Time Filters using Nonlinear Sequence Transformation" and submitted by Goutham Makkena ID No. 2009PH230002H for award of Ph.D. of the Institute embodies original work done by him under my supervision.

Supervisor
Dr. M. B. Srinivas
Professor,
BITS-Pilani, Hyderabad Campus
Date:

Acknowledgements

I wish to express sincere gratitude to my supervisor Prof. M. B. Srinivas for his help and valuable guidance, without which this work would not have been accomplished. His unwavering support through out the journey has been a constant source of encouragement. I am grateful to Prof. G. Sundar, Director, Birla Institute of Technology and Science - Pilani, Hyderabad Campus for providing all the necessary facilities required to conduct my research. I also take this opportunity to thank the previous and current Heads of the Department of Electrical Engineering, Prof. Y. Yoganandam and Prof. Sanket Goel respectively for the support and help extended to me. I would also like to thank my Doctoral Advisory Committee (DAC): Prof. Prabhakara Rao and Prof. S. K. Chatterjee, for their timely feedback and insightful comments. To all my friends in the department, thank you for your cooperation and camaraderie - especially to Mr. Sai Phaneendra Parlapalli, Mr. Chetan Kumar Vudadha and Mr. Avinash S Vaidya for helping me overcome difficult phases and not letting me give up. Lastly, my warmest acknowledgements to my parents, sister and my wife for being there for me all the time.

Abstract

Advanced filtering techniques like wavelet filters and linear-phase frequency selective filters consume very low power when implemented as continuous-time filters. Both these filters have prescribed impulse responses and hence can be easily synthesized in time-domain. A key step in the time-domain synthesis of a continuous-time filter is the approximation of its transfer function to a proper rational function. In this thesis, a closed-form method known as nonlinear sequence transformation is used to obtain rational approximation of these advanced filters.

Nonlinear sequence transformation utilizes regularities in a slowly converging infinite series, like the Taylor expansion, to accomplish convergence acceleration by transforming it to a rational function. Of the many variants of nonlinear sequence transformation, Levin and Weniger transformations are being extensively used. However, direct application of the versions of Levin and Weniger transforms falls short in obtaining BIBO stable proper rational approximations for wavelet filters. Hence, new variants of nonlinear sequence transformation that obtain BIBO stable rational approximations for wavelet filters is proposed in this thesis. These variants perform better in terms of mean square error when compared to those obtained by other closed-form methods. It is shown that the model order reduction of the proposed variants leads to either similar or better performance compared to L_2 optimization method. These variants

are also shown to act as good starting points for optimization methods that use local search routines.

In this thesis, a new closed-form solution for the design of linear-phase selective filters is presented. The approach consists of developing an approximation to the Laplace transform of impulse response of the chosen linear-phase selective filter using a sum of shifted and scaled causal splines. This approximation is then rationalized using the proposed variants of nonlinear sequence transformation to obtain a realizable medium order transfer function which is then balanced and truncated to the required order. The magnitude and phase features of the filter derived are presented and discussed. It is shown that the closed-form solution obtained can act as a starting point for approximation methods that use local search routines.

Finally, a transfer function obtained by one of the proposed variants is converted to an equivalent electrical network and is simulated to show that the proposed variants are implementable. The electrical network is obtained in the form of a G_m-C circuit which approximates a Gabor wavelet. From the simulation results, it is clear that the circuit has the required characteristics of a Gabor wavelet filter.

Contents

Certificate i

Acknowledgements ii

Abstract iii

Contents v

List of Figures ix

List of Tables xiii

Abbreviations xv

1 Introduction 1

1.1 Time-domain Synthesis 1

1.2 Continuous-Time Filters 3

1.3 Time-domain synthesis of continuous-time filters 4

1.4 Approximation Methods 6

1.5 Objectives of the Thesis 9

1.6 Organization of the Thesis 10

2 Nonlinear Sequence Transformation **11**

2.1 Nonlinear Sequence Transformation 12

2.2 Levin's Transformations 15

2.3 Weniger's Transformations 19

2.4 Gaussian Filter Approximation Using Levin & Weniger Transformations 21

2.4.1 Mathematical Representation 21

2.4.2 Approximation of Gaussian Filter Transfer Function 22

2.5 Conclusion 30

3 Approximation of Nonlinear Sequence Transformation-based Continuous-Time Wavelet Filter **31**

3.1 Nonlinear Sequence Transformation and Problem with leading irregular Taylor coefficients 35

3.2 Proposed Variants to Obtain Proper Rational Approximations for Wavelets with Leading Irregular Taylor Coefficients 38

3.2.1 Choice of the parameters p and β 42

3.2.2 Rational approximation and admissibility property 44

3.3 Approximation of Different Wavelet Bases using Proposed Variants . . 45

3.4 Performance Evaluation 50

3.4.1 Comparison with Padé Method 50

3.4.2 Comparison with the L_2 Method 52

3.4.3 Proposed Variants as Alternate Starting Points 55

3.5 Conclusion 57

4 Closed-Form Design of Continuous-Time Linear-Phase Selective Filters 58

4.1 Causal B-splines 60

4.2 Proposed Method 62

4.2.1 Magnitude and Phase properties of the Proposed Filter 65

4.3 Properties of the Proposed Filters 68

4.4 Comparison With L_2-Method 72

4.5 Proposed Method as a Starting Point 74

4.6 Conclusion 75

5 Circuit Implementation 76

5.1 Circuit Implementation of Gabor Wavelet 77

5.2 Filter design 81

5.3 Low power transconductor circuit design 82

5.4 Simulation Results 83

5.5 Conclusion 86

6 Conclusions and Future Work **87**

6.1 Future Work 89

Bibliography **90**

List of Figures

1.1 A LTI system with the required impulse response 2

1.2 Major steps involved in time-domain filter synthesis 3

1.3 Two approaches to the approximation in time-domain synthesis 6

2.1 Variation of MSE with β for 5^{th} order approximation of the u, t, y and τ transformations for a Gaussian pulse ($\sigma = 0.5$, $\mu = 2$) 24

2.2 Pole-Zero plots of the Gaussian transfer functions 25

2.3 Gaussian impulse response approximation using u-transformation. . . . 26

2.4 Gaussian impulse response approximation using t-transformation. . . . 27

2.5 Gaussian impulse response approximation using y-transformation. . . . 28

2.6 Gaussian impulse response approximation using τ-transformation. . . . 29

3.1 Absolute percentage change of Taylor Coefficients $a_0 - a_5$ of Gaussian wavelet as the translation is increased 37

3.2 Location of Poles on the complex plane as n is varied for a 5^{th} order u-transformation approximation of Gaussian wavelet ($t_0 = 2$, $\sigma = 1$) . . 37

3.3 Variation of MSE with β for 5^{th} order approximation of the proposed variants (p=1) for a Gaussian wavelet ($t_0 = 2$, $\sigma = 1$) 46

3.4 Wavelet base approximations carried out using the proposed variants. The thick gray line is the wavelet and the dashed black line is the impulse response of the approximated wavelet. Following wavelets are approximated with orders $O()$ and time shifts $T()$: (the scale σ is 1 unless specified otherwise) (a) Gaussian Wavelet $O(5), T(2)$ (b) Mexican Hat Wavelet $O(7)$,$T(3)$ (c) Compactly supported Spline Wavelet of order 2 O(8) T(0) (d) 3^{rd} derivative of B-Spline of order 7, $O(9), T(0)$, $\sigma = 0.5$ (e) 4^{th} derivative of Exponential-Spline of order 8, $\alpha = 0.25$, $O(9), T(0)$ (f) Morlet Wavelet (Gaussian multiplied by cosine of angular frequency $6rad/sec$),$O(10), T(3)$. 48

3.5 MSE versus order of approximation for Padé and Proposed variants for (a) Gaussian Wavelet ($t_0 = 2, \sigma = 1$) (b) Mexican Hat Wavelet ($t_0 = 3, \sigma = 1$) (c) Third derivative of seventh order B-spline ($t_0 = 0, \sigma = 0.5$) (d) Fourth derivative of eighth order Exponential spline ($t_0 = 0, \sigma = 1, \alpha = 0.25$) 51

3.6 MSE versus order of approximation for L_2 method, model reduced proposed variant and best among the proposed variants (a) Gaussian Wavelet ($t_0 = 2, \sigma = 1$) (b) Mexican Hat Wavelet ($t_0 = 3, \sigma = 1$) (c) Third derivative of seventh order B-spline ($t_0 = 0, \sigma = 0.5$) (d) Fourth derivative of eighth order Exponential spline ($t_0 = 0, \sigma = 1, \alpha = 0.25$) . 54

3.7 MSE versus order of approximation for L_2 method with proposed variant and method described in [1] as starting points (a) Gaussian Wavelet ($t_0 = 2, \sigma = 1$) (b) Mexican Hat Wavelet ($t_0 = 3, \sigma = 1$) (c) Third derivative of seventh order B-spline ($t_0 = 0, \sigma = 0.5$) (d) Fourth derivative of eighth order Exponential spline ($t_0 = 0, \sigma = 1, \alpha = 0.25$) 56

4.1 Required Symmetric Sinc pulse with delay T_0 and cut-off frequency ω_c = 1 rad/sec. 63

4.2 Magnitude and Phase response of the proposed transfer function for p=4 (a) Magnitude response (b) Phase response 67

4.3 Magnitude and responses of proposed filter normalized to $\omega_c = 1$ rad/sec (a) Magnitude responses for orders $4, 5$ and 6 (b) Magnitude responses for orders $7, 8$ and 9 (c) Magnitude responses for orders $10, 11$ and 12 (d) Phase responses for orders 4 to 12 70

4.4 Impulse responses of the proposed filter (a) Orders $4, 5$ and 6 (b) Orders 7 and 8 (c) Orders 9 and 10 (d) Orders 11 and 12 71

4.5 Comparison of the proposed method with L_2 method (a) 5^{th} order magnitude responses (b) 7^{th} order magnitude responses (c) 9^{th} order magnitude responses (d) Phase response comparison for orders 5, 7 and 9 73

4.6 Comparison of responses of the 9^{th} order filters after L_2 optimization using different starting points (a) Magnitude response (b) Phase response. 75

5.1 Impulse responses of the Gaussian window, the ideal impulse(solid line) and the approximated impulse(dashed line). 79

5.2 Impulse response approximation: Imaginary output 80

5.3 Impulse response approximation: Real output 81

5.4 Schematic of the transconductor. 82

5.5 Block diagram of the Gabor wavelet-transform filter (Real Part). 84

5.6 Magnitude response comparison of the designed filter with respect to magnitude response of the transfer function 85

List of Tables

3.1 Zeros and Poles of 5^{th} order Approximations of Gaussian wavelet and Mexican Hat wavelet Obtained by different variants of Nonlinear sequence transformation 36

3.2 Variation of minimum MSE as p is varied for $\widehat{u}$-transformation approximation of Gaussian wavelet. (the corresponding β value for which the mininum MSE occurs is given in braces) 46

3.3 Variation of minimum MSE as p is varied for $\widehat{t}$-transformation approximation of Gaussian wavelet. (the corresponding β value for which the mininum MSE occurs is given in braces) 47

3.4 Variation of minimum MSE as p is varied for $\widehat{y}$-transformation approximation of Gaussian wavelet. (the corresponding β value for which the mininum MSE occurs is given in braces) 47

3.5 Variation of minimum MSE as p is varied for $\widehat{\tau}$-transformation approximation of Gaussian wavelet. (the corresponding β value for which the mininum MSE occurs is given in braces) 47

3.6 Effect of the time shift on the Order of approximation, MSE and Energy Loss for the $\widehat{\tau}$-transformation when approximating Gaussian wavelet (σ =1) 49

3.7 Proposed variant, its order and corresponding p and β values used for model reduction for different wavelets 53

4.1 The values of p and the medium order $k_{n,m}$ 68

5.1 Summary of simulated filter performance 85

Abbreviations

LTI	**L**inear **T**ime **I**nvariant
WT	**W**avelet **T**ransform
dB	**D**ecibels
pW	**P**ico **W**atts
nW	**N**ano **W**atts
μ**W**	**M**icro **W**atts
ADC	**A**nalog to **D**igital **C**onverter
DAC	**D**igital to **A**nalog **C**onverter

Chapter 1

Introduction

1.1 Time-domain Synthesis

Traditionally, analog filter design concerned itself with approximation of the required characteristics using polynomials and rational functions as functions of frequency. Accordingly, filters such as Butterworth, Chebyshev, Elliptic, Cauer, Legendre which approximate the rectangular magnitude either in maximally flat or equiripple sense were developed [2]. However, as communications and signal processing fields evolved, requirement for electrical networks that had specific transient responses arose. This lead to research on *synthesis of time-domain filters* in the 1950's [3–20].

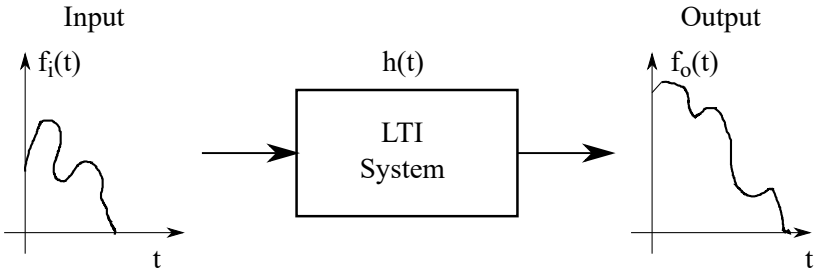

Figure 1.1: A LTI system with the required impulse response

Time-domain synthesis of filters consists of three steps. In the first step, the input function $f_i(t)$ of the filter, also known as the excitation function and the desired output function $f_o(t)$, also known as the response function are identified as shown in Figure. 1.1. Impulse response, denoted by $h(t)$, that corresponds to this input-output pair is then identified because the input function $f_i(t)$ and the desired output function $f_o(t)$ are related by the equation given below:

$$f_o(t) = f_i(t) * h(t) \tag{1.1}$$

The star in the above equation denotes convolution.

The second step consists of obtaining transfer function $H(s)$ of the linear time-invariant (LTI) system whose inverse transform closely approximates the impulse response $h(t)$ in equation (1.1). This approximation has to be in an appropriate form, i.e, a proper rational function with numerator and denominator polynomials having real coefficients while the denominator polynomial is strictly Hurwitz. The third step consists of practical implementation of the approximated transfer function $H(s)$ in the

form of an electrical network.

In this work we focus on the second step of the three steps outlined i.e, the approximation of the transfer function $H(s)$ to a practically realizable form as shown in figure 1.2.

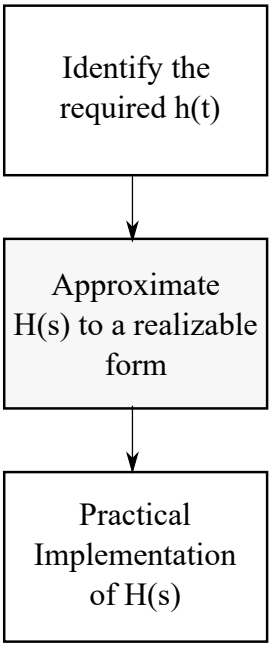

Figure 1.2: Major steps involved in time-domain filter synthesis

1.2 Continuous-Time Filters

Filters are primarily implemented as electrical networks consisting of lumped elements operating on continuous-time analog signals. As the field of VLSI and Microprocessors evolved, filters that can operate on sampled, discrete-time signals called digital filters have been developed. These filters usually contain analog-to-digital converters (ADCs)

to sample the input signal, followed by a device such as a microcontroller to perform mathematical operations and finally a digital-to-analog converter(DAC) at the output. The introduction of ADC, microcontrollers and DAC might result in an expensive filter when compared to an equivalent analog filter. However digital filters make complex designs practical that are not possible with analog filters. This made digital filters ubiquitous in everyday devices like computers, radios, televisions etc [21].

However, signal processing in continuous-time domain is still preferred where power consumption is a critical design constraint (Eg: devices that are powered by battery). Power consumption is even more critical in implantable devices, wherein the battery cannot be recharged. Advanced signal processing techniques when implemented as continuous-time filters consume very low power, of the order of nW and hence are very much suited to low power applications.

1.3 Time-domain synthesis of continuous-time filters

Time-domain synthesis has been used successfully to design continuous-time filters in case of wavelet filters [1, 22, 23], linear-phase selective filters [24–26], pulse forming and shaping networks[27–29] etc.

Wavelet Transform [30–32] has evolved as a powerful tool for analysis of non-stationary signals owing to it's time frequency localizations. Continuous Wavelet Transform (CWT) has proven to be highly useful technique in this respect. In CWT, the signal to be analyzed is convolved with scaled copies of basis functions called mother wavelets. This allows for a signal under study to be mapped to a time-scale plane in which the spectral content of a signal with respect to time is obtained thereby aiding in feature detection. It is shown in [22, 23, 33–37] that Wavelet Transform implemented as CWT in analog domain consumes ultra low power in the range of pW.

Linear-phase selective filters are used extensively when there is a requirement for both rectangular magnitude and linear phase response. Such filters are used extensively when group-delay equalization is required [38, 39]. Successful time-domain synthesis of linear-phase selective continuous-time filters has been presented in [24–26].

A key step in time-domain synthesis of the above mentioned wavelet filters and linear-phase selective filters is the rational approximation of the transfer function of linear time invariant system, whose impulse response is the required wavelet and sinc pulse respectively. This thesis focuses on this key approximation step to synthesize wavelet and linear-phase selective filters.

1.4 Approximation Methods

There are two major approaches to the approximation problem (second step in figure. 1.2) in time-domain synthesis, which are shown in the figure below:

The first approach obtains the approximated transfer function $H^*(s)$ by approximating

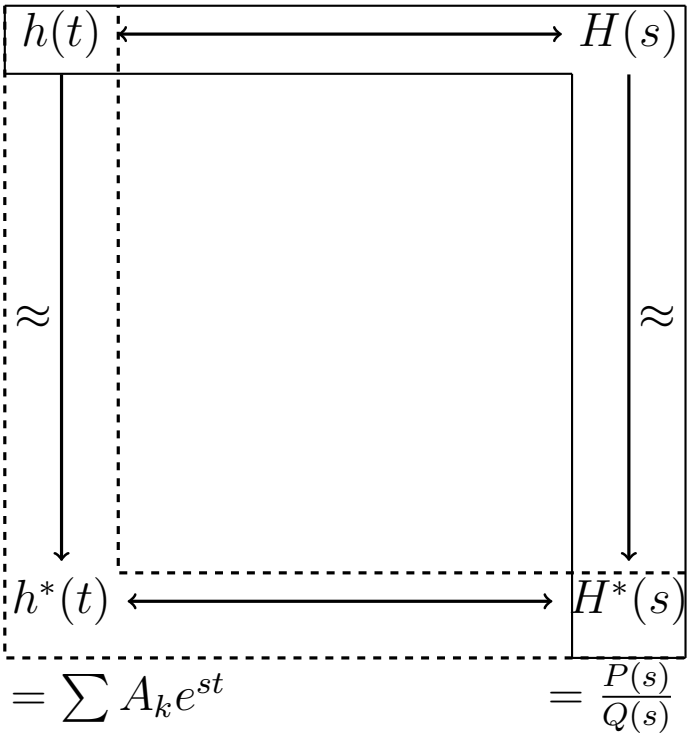

Figure 1.3: Two approaches to the approximation in time-domain synthesis

the desired impulse response $h(t)$ as a sum of damped exponentials and complex exponentials $h^*(t)$ as shown in equation (1.2)

$$h^*(t) = \alpha_1 e^{p_1 t} + \beta_1 e^{(q_1+ir_1)t} + \beta_1^* e^{(q_1-ir_1)t} + \beta_2 e^{(q_2+ir_2)t} + \beta_2^* e^{(q_2-ir_2)t} \tag{1.2}$$

Then, approximation techniques that are based on certain error criteria between the desired and approximated response are used to minimize the error. The most commonly used error criteria is the mean square error (MSE) approximation given by

$$MSE = \int_{-\infty}^{\infty} |h(t) - h^*(t)|^2 \, dt \tag{1.3}$$

This equation is minimized using several optimization procedures such as nonlinear least squares [40], second-order cone programming [25], differential evaluation algorithm [41], simulated annealing [42], particle swarm optimization [43], chaotic map particle swarm optimization with local sequential quadratic programming [44] etc. This approach is depicted by the dotted lines in figure 1.3.

In the second approach, initially the desired transfer function $H(s)$ is obtained by calculating the Laplace transform of the desired impulse response $h(t)$. It is then expressed as truncated power series with the help of expansions such as Taylor series, McLaurin series etc. The truncated Taylor series expansion of $H(s)$ typically looks like

$$H(s) = a_0 + a_1 s + a_2 s^2 + a_3 s^3 + \cdots + a_k s^k \tag{1.4}$$

where a_0, a_1, a_2, a_3 $\cdots a_k$ are the Taylor coefficients. This truncated expansion is converted to a proper rational function by techniques like Padé approximation [45].

Padé approximation converts a power series of $H(s)$ into a doubly indexed sequence of rational function given by

$$H(s) = \frac{P^m(s)}{Q^n(s)} = \frac{p_0 + p_1 s + \cdots + p_m s^m}{1 + q_1 s + \cdots + q_n s^n} \tag{1.5}$$

The co-efficients $p_0, p_1, ..., p_m$ and $q_1, q_2, ..., q_n$ are obtained such that the Taylor expansion of P/Q at $s = 0$ agrees with the power series as much as possible.

$$Q^n(s)H(s) - P^m(s) = O(s^{m+n+1}), \qquad s \to 0 \tag{1.6}$$

This equation above gives rise to $m + n + 1$ linear equations. If this system has a solution, then it leads to coefficients of $P^m(s)$ and $Q^n(s)$.
The second approach is depicted by the solid lines in figure 1.3.

A careful observation of these approximation methods lets us to classify these methods broadly as optimization methods and closed-form methods. Optimization methods use several iterative routines [25, 40–44], where as the closed-form methods use definitive procedures [27, 45, 46]. Optimization routines let designers handle several constraints during the approximation procedure. They also let the designer come up with a solution that meets a required MSE. However, since most of the optimization routines employ iterative procedures, the solution arrived at often is a local optimum. For some iterative procedures, the starting points considered greatly affect the final approximation. Even though optimization methods are effective, closed-form methods

are attractive because they are straight-forward and easy to design.

1.5 Objectives of the Thesis

While there are several optimization procedures used in the time-domain approximation problem [25, 40–44], very few generic closed-form methods [45] are available in the literature. Thus, the objectives of this thesis are as follows:

- Develop a closed-form technique that can solve the approximation problem in time-domain synthesis.
- Apply this technique and approximate several mother wavelet bases to compare with existing methods
- Approximate linear-phase selective filters using this technique and compare with existing methods
- Demonstrate that the transfer function obtained by the proposed method can be implemented as a circuit to validate the technique.

1.6 Organization of the Thesis

This thesis is organized as follows. Chapter 2 introduces a closed-form approximation method namely nonlinear sequence transformation. It also shows that this technique can be successfully used to approximate Gaussian filters. In the third chapter it is shown that the nonlinear sequence transformation technique when applied on wavelets does not produce stable transfer functions and hence proposes a modified technique to obtain stable transfer functions for wavelet filters. Chapter 4 develops a new expression for the Laplace transform of a linear-phase selective filter before applying the modified technique proposed in Chapter 3 to obtain stable rational transfer functions. Chapter 5 implements one of the transfer functions obtained by the proposed variants of nonlinear sequence transformation as a operational transconductance amplifier - capacitor (OTA-C) circuit to validate the techniques developed. Chapter 6 gives conclusions and directions for future work.

Chapter 2

Nonlinear Sequence Transformation

Power series, like the one shown in equation 1.4 mentioned earlier, is an important tool in mathematics owing to its analytical properties and is used to mathematically treat several scientific and engineering problems. Summing up a power series that converges slowly is an age old problem that occurs in many fields of science and engineering. Convergence acceleration of series using extrapolation techniques based on linear and nonlinear sequence transformation, has been researched heavily and is present in the literature in the form of exclusive monographs [47–54] and in sections of books on numerical computing [55–57].

2.1 Nonlinear Sequence Transformation

Nonlinear sequence transformation starts with assuming that a slowly convergent or divergent sequence $\{S_n\}_{n=0}^{\infty}$, where S_n contains partial sums of infinite series as,

$$S_n = \sum_{k=0}^{n} a_k \tag{2.1}$$

can be partitioned into a generalized limit S and a remainder or a truncation error r_n given by

$$S_n = S + r_n \tag{2.2}$$

An infinite series is typically evaluated by adding many of its terms such that the remainder r_n becomes negligible. However, this approach is not feasible because only so many terms of the sequence can be added owing to practical limitations. An alternate approach to evaluate such series would be to approximate the remainder r_n and eliminate it from the sequence elements S_n. A sequence transformation tries to accomplish this by transforming a given sequence $\{S_n\}_{n=0}^{\infty}$ to a new sequence $\left\{\widetilde{S_n}\right\}_{n=0}^{\infty}$ that has the same generalized limit S but a different remainder $\widetilde{r_n}$.

$$\widetilde{S_n} = S + \widetilde{r_n} \tag{2.3}$$

The transformed sequence given in the above equation is said to be successful if the new remainder $\widetilde{r_n}$ converges much faster compared to the actual remainder r_n given as

$$\lim_{n\to\infty} \frac{\widetilde{r_n}}{r_n} \quad = \quad \lim_{n\to\infty} \frac{\widetilde{S_n} - S}{S_n - S} \quad = \quad 0 \tag{2.4}$$

It is often not feasible to find the numerical values of the remainders r_n and thus sequence transformations obtain approximations to the remainders by using the *structural information* of the sequence to be transformed. This is explained with the help of an example give below.

Consider a sequence S_n which contains partial sums of a strictly alternating series given by

$$S_n = \sum_{k=0}^{n} (-1)^k b_k \tag{2.5}$$

where all values of b_n, $n \in \mathbb{N}_0$ have the same sign. The remainder r_n of this sequence S_n can now be written as

$$r_n = -\sum_{k=n+1}^{\infty} (-1)^k b_k. \tag{2.6}$$

Let us now assume that the series converges to a limit S, which implies that the values of b_n, $n \in \mathbb{N}_0$ are positive and decreasing as n is increasing and finally vanish as $n \to \infty$. This also results in the magnitude of the remainder r_n being bound by its first term,

i.e, b_{n+1} which is not a part of the sequence S_n [58] and is given as

$$|r_n| < b_{n+1}, \quad n \in \mathbb{N}_0. \tag{2.7}$$

The above inequality gives *structural information* about the remainder r_n by expressing the ratio $r_n/[(-1)^{n+1}b_{n+1}]$ as an asymptotic power series in the variable $1/(n+1)$ i.e,

$$r_n = (-1)^{n+1}b_{n+1}\sum_{j=0}^{\infty} c_j(n+1)^{-j}, \qquad n \to \infty \tag{2.8}$$

However, elimination of the remainder r_n given in the above equation by computing the infinite asymptotic series is not possible and hence model remainders of the below type are considered

$$\widetilde{r_n} \approx (-1)^{n+1}b_{n+1}\sum_{j=0}^{k} c_j(n+1)^{-j}, \qquad n \in \mathbb{N}_0 \tag{2.9}$$

For sufficiently large values of k and n, the new remainder $\widetilde{r_n}$ approximates the actual remainder r_n closely. This implies that the sequence S_n also can be approximated by the new remainder $\widetilde{r_n}$, which contains only finite terms as:

$$\widetilde{S_n} = S + (-1)^{n+1}b_{n+1}\sum_{j=0}^{k} c_j(n+1)^{-j}, \qquad n \in \mathbb{N}_0 \tag{2.10}$$

Nonlinear sequence transformation utilizes regularities in a slowly converging infinite series to accomplish convergence acceleration by transforming it to a rational function

[47]. This convergence acceleration is a result of extrapolation of the rational function obtained thus eliminating the need for asymptotic approximations which require heavy computations.

2.2 Levin's Transformations

The best-known example of sequence transformation is the Levin's transformation [59] widely used for convergence acceleration of infinite series. It has been extensively used to accelerate spectral domain immitance [60–64] and in electromagnetic modeling of high-speed interconnects [65]. Levin's transformation starts with the assumption that the series, $S_n(s) = \sum_{i=0}^{n-1} a_i s^i$, where a_i $(i = 0 \text{ to } n-1)$ are the terms of the series, admits

$$S_n = S + \omega_n \sum_{j=0}^{k-1} \frac{c_j}{(n+\beta)^j}, \qquad k, n \in \mathbb{N}_0 \tag{2.11}$$

for certain values of the parameters $\{c_n\}_0^{k-1}$. It is to be noted that S is the generalized limit, ω_n is a remainder estimate and β is a constant shift parameter. Multiplying both sides by $(n+\beta)^{k-1}$ would yield

$$\frac{S_n - S}{\omega_n}(n+\beta)^{k-1} \quad = \quad \sum_{j=0}^{k-1} c_j (n+\beta)^{k-j-1} \quad = \quad P_{k-1}(n) \tag{2.12}$$

The Right Hand Side (RHS) of (2.12) is a polynomial in n of order $k-1$ ($P_{k-1}(n)$), which can be completely annihilated by the forward difference operator of order k (Δ^k). Applying Δ^k we obtain the k^{th} order Levin transformation as a rational approximation to S as,

$$S = \frac{\sum_{j=0}^{k}(-1)^j\binom{k}{j}(n+j+\beta)^{k-1}\frac{S_{n+j}}{\omega_{n+j}}}{\sum_{j=0}^{k}(-1)^j\binom{k}{j}(n+j+\beta)^{k-1}\frac{1}{\omega_{n+j}}} \tag{2.13}$$

The Δ operator property

$$\Delta^k f(n) = \sum_{j=0}^{k}(-1)^j\binom{k}{j}f(n+j) \tag{2.14}$$

is used to obtain the equation (2.13).

Different choices of the remainder estimate ω_n result in different variants of Levin's transformation. Levin's u-transformation is obtained by substituting $\omega_n = (n+\beta)\Delta S_{n-1}$ in equation (2.13) leading to

$$u = \frac{\sum_{j=0}^{k}(-1)^j\binom{k}{j}(n+j+\beta)^{k-2}\frac{S_{n+j}}{\Delta S_{n+j-1}}}{\sum_{j=0}^{k}(-1)^j\binom{k}{j}(n+j+\beta)^{k-2}\frac{1}{\Delta S_{n+j-1}}} \tag{2.15}$$

Using equation (2.14), the value of ΔS_{n+j-1} can be calculated and is given as,

$$\Delta S_{n+j-1} = a_{n+j-1} s^{n+j-1} \tag{2.16}$$

Substituting the above equation and the actual series $S_{n+j} = \sum_{i=0}^{n+j-1} a_i s^i$ in equation (2.16), we obtain

$$u = \frac{\sum_{j=0}^{k} \sum_{i=0}^{n+j-1} (-1)^j \binom{k}{j} (n+j+\beta)^{(k-2)} \left(\frac{a_i s^i}{a_{n+j-1} s^{n+j-1}} \right)}{\sum_{j=0}^{k} (-1)^j \binom{k}{j} (n+j+\beta)^{(k-2)} \left(\frac{1}{a_{n+j-1} s^{n+j-1}} \right)} \tag{2.17}$$

By changing the index of summation of the denominator in equation (2.17) using the identity $\sum_{j=0}^{k} a_j = \sum_{j=0}^{k} a_{k-j}$, we obtain

$$u = \frac{\sum_{j=0}^{k} \sum_{i=0}^{n+j-1} (-1)^j \binom{k}{j} (n+j+\beta)^{(k-2)} \left(\frac{a_i s^i}{a_{n+j-1} s^{n+j-1}} \right)}{\sum_{j=0}^{k} s^j (-1)^{k-j} \binom{k}{j} (n+k-j+\beta)^{(k-2)} \left(\frac{1}{a_{n+k-j-1} s^{n+k-1}} \right)} \tag{2.18}$$

Now, changing the limits of the double finite summation present in the numerator of equation (2.18) using the identity $\sum_{j=0}^{k} \sum_{i=0}^{n+j-1} a_{j,i} = \sum_{i=0}^{n+k-1} \sum_{j=i-(n-1)}^{k} a_{j,i}$ results in

$$u = \frac{\sum_{i=0}^{n+k-1} \sum_{j=i-(n-1)}^{k} (-1)^j \binom{k}{j} (n+j+\beta)^{(k-2)} \left(\frac{a_i s^i}{a_{n+j-1} s^{n+j-1}} \right)}{\sum_{j=0}^{k} s^j (-1)^{k-j} \binom{k}{j} (n+k-j+\beta)^{(k-2)} \left(\frac{1}{a_{n+k-j-1} s^{n+k-1}} \right)} \tag{2.19}$$

Now, changing the index of summation of the numerator involving j in equation (2.19) using the identity $\sum_{j=i-(n-1)}^{k} a_j = \sum_{j=i-(n-1)}^{k} a_{k-j+i-(n-1)}$,

$$u = \frac{\sum_{i=0}^{n+k-1} \sum_{j=i-(n-1)}^{k} (-1)^{k-j+i-(n-1)} \binom{k}{k-j+i-(n-1)} (n+k-j+i-(n-1)+\beta)^{(k-2)} \left(\frac{a_i s^i}{a_{n+k-j+i-(n-1)-1} s^{n+k-j+i-(n-1)-1}} \right)}{\sum_{j=0}^{k} s^j (-1)^{k-j} \binom{k}{j} (n+k-j+\beta)^{(k-2)} \left(\frac{1}{a_{n+k-j-1} s^{n+k-1}} \right)} \tag{2.20}$$

By changing the limits of the double summation of (2.20) again we get

$$u = \frac{\sum_{j=0}^{k} s^j \sum_{i=0}^{n+j-1} (-1)^{k-j+i-(n-1)} \binom{k}{k-j+i-(n-1)} (n+k-j+i-(n-1)+\beta)^{(k-2)} \left(\frac{a_i s^i}{a_{n+k-j+i-(n-1)-1} s^{n+k+i-(n-1)-1}} \right)}{\sum_{j=0}^{k} s^j (-1)^{k-j} \binom{k}{j} (n+k-j+\beta)^{(k-2)} \left(\frac{1}{a_{n+k-j-1} s^{n+k-1}} \right)} \tag{2.21}$$

The final expression for the u-transformation can now be obtained by changing the index of the summation involving i in the numerator of equation (2.21) as,

$$u = \frac{\sum_{j=0}^{k} s^j \sum_{i=0}^{n+j-1} (-1)^{k-i} \binom{k}{i} (n+k-i+\beta)^{(k-2)} \left(\frac{a_{n-1+j-i}}{a_{n-1+k-j}} \right)}{\sum_{j=0}^{k} s^j (-1)^{k-j} \binom{k}{j} (n+k-j+\beta)^{(k-2)} \left(\frac{s^{1-n}}{a_{n-1+k-j}} \right)} \tag{2.22}$$

Similarly, a choice of $\omega_n = \Delta S_{n-1}$ in equation (2.13) gives Levin's t-transformation. Following the procedure described through equations (2.15)-(2.21) gives the final

expression for the t-transformation as

$$t = \frac{\sum_{j=0}^{k} s^j \sum_{i=0}^{n+j-1} (-1)^{k-i} \binom{k}{i} (n+k-i+\beta)^{(k-1)} \left(\frac{a_{n-1+j-i}}{a_{n-1+k-j}}\right)}{\sum_{j=0}^{k} s^j (-1)^{k-j} \binom{k}{j} (n+k-j+\beta)^{(k-1)} \left(\frac{s^{1-n}}{a_{n-1+k-j}}\right)} \tag{2.23}$$

2.3 Weniger's Transformations

The Levin's transformation derived was for the model sequences of the type described by equation (2.11). A new class of sequence transformations called the Weniger's transformations is derived when model sequences of the type given in the equation below are considered

$$S_n = S + \omega_n \sum_{j=0}^{k-1} \frac{c_j}{(n+\beta)_j}, \qquad k, n \in \mathbb{N}_0 \tag{2.24}$$

The difference between equation (2.11) and equation (2.24) is that the powers $(n+\beta)^k$ in Levin transformation are replaced by Pochhammer symbols $(n+\beta)_k$ in Weniger transformation. Following the same process as described in the previous section, we can obtain different variants of Weniger transformation. A choice of $\omega_n = (n+\beta)\Delta S_{n-1}$ and $\omega_n = \Delta S_{n-1}$ gives Weniger's y and τ-transformations respectively and their final

expressions are given below as

$$y = \frac{\sum_{j=0}^{k} s^j \sum_{i=0}^{n+j-1} (-1)^{k-i} \binom{k}{i} (n+k-i+\beta)_{(k-2)} \left(\frac{a_{n-1+j-i}}{a_{n-1+k-j}} \right)}{\sum_{j=0}^{k} s^j (-1)^{k-j} \binom{k}{j} (n+k-j+\beta)_{(k-2)} \left(\frac{s^{1-n}}{a_{n-1+k-j}} \right)} \tag{2.25}$$

$$\tau = \frac{\sum_{j=0}^{k} s^j \sum_{i=0}^{n+j-1} (-1)^{k-i} \binom{k}{i} (n+k-i+\beta)_{(k-1)} \left(\frac{a_{n-1+j-i}}{a_{n-1+k-j}} \right)}{\sum_{j=0}^{k} s^j (-1)^{k-j} \binom{k}{j} (n+k-j+\beta)_{(k-1)} \left(\frac{s^{1-n}}{a_{n-1+k-j}} \right)} \tag{2.26}$$

Equations (2.22)-(2.23) describe the Levin transformations and (2.25)-(2.26) describe the Weniger transformations. From these expressions, two key observations can be made:

(i) For a given value of k, the value of the parameter n defines the minimal index of the partial sums used in these approximations. That is, if $n = 1$, the partial sums S_0 to S_k are used in the rational approximation.

(ii)The order of approximation is given as $\frac{k+n-1}{k}$, for a given value of k

2.4 Gaussian Filter Approximation Using Levin & Weniger Transformations

Gaussian filter is a filter whose impulse response is Gaussian. It is used in digital communications to limit the spectral energy outside the transmission band [66]. It is also used on physiological signals for smoothening. Another important application of Gaussian filter is modeling analog delays [67]. Analog delays are achieved by Gaussian filters which are obtained by approximating very thin Gaussian functions. Gaussian filters are usually implemented in digital domain which however use power hungry elements such as Digital-to-Analog Converter (DAC) and Voltage Controlled Oscillator (VCO). When implemented in analog domain, Gaussian filter consumes very low power compared to its digital counterpart. However to obtain Gaussian filter in analog domain, a faithful approximation of the Gaussian function is required.

2.4.1 Mathematical Representation

Gaussian filter convolves the input signal with a Gaussian function. This process of convolution of a signal with a Gaussian function is also called as the Weierstrass transform. Equation (2.27) below shows the Gaussian function, where μ is the time-shift

and σ is the scale.

$$f(t) = \frac{1}{\sigma\sqrt{2\pi}} e^{\frac{-(t-\mu)^2}{2\sigma^2}} \tag{2.27}$$

A given transfer function $H(s)$ is called a Gaussian filter, if its impulse response follows a given Gaussian closely [67].

When an attempt is made to find the Laplace Transform of the Gaussian function given in equation (2.27), we encounter integrals which are transcendental in nature. For example, for a Gaussian function $f(t)$ with time-shift $\mu = 2$ and scale $\sigma = 1$, the Laplace Transform $F(s)$ is,

$$F(s) = 0.06766764162\, \mathrm{e}^{\frac{(s-2.0)^2}{2}} \operatorname{erfc}\left(\sqrt{2}\left(\frac{s}{2} - 1.0\right)\right) \tag{2.28}$$

where erfc(s) is the complementary error function. Clearly, equation (2.28) is not a strictly proper rational function with all poles having negative real parts, the necessary condition for a practically realizable transfer function.

2.4.2 Approximation of Gaussian Filter Transfer Function

As seen from equation (2.28), a necessity arises for transfer functions in transcendental form to be approximated as proper rational functions. The series expansions of most of these transcendental functions can be obtained at points like $s = 0$, which can

then be rationalized using Levin and Weniger transformations given by the equations (2.22)-(2.23) and (2.25)-(2.26) respectively. The value of n in the (2.22)-(2.23) and (2.25)-(2.26) has to be taken as 1 so as to obtain proper rational approximations. The other parameters in those equations are k, which is the order of the approximation, the Taylor coefficients a_k and the constant shift parameter β. A minimum value for β can be chosen from the following inequality.

$$\beta \; > \; -(1) \tag{2.29}$$

This is obtained from the fact that the factor $(1 + k - j + \beta)$ in equations (2.22)-(2.23) and (2.25)-(2.26) should always be positive.

As the value of β is varied around this minimum value, the impulse response also varies, which is different for different variants. Each variant has it's own value of β for which the impulse response obtained has a minimum mean square error (MSE) with reference to the actual Gaussian pulse. Figure 2.1 shows the variation of mean square error of the 5^{th} order approximation of the Gaussian ($\sigma = 0.5$, $\mu = 2$) as β is varied.

Once the value of β, for which minimum MSE is obtained, is identified, that value is used to calculate the final transfer function of the Gaussian pulse. The 5^{th} order approximations of the Gaussian pulse ($\sigma = 0.5$, $\mu = 2$), for example, obtained with the u, t, y and τ-transformations are given by equations (2.30)-(2.33) and shown in Figures 2.3(a) - 2.6(a) respectively. Figures 2.2(a)-2.2(d) show the pole-zero locations

of these transfer functions. From these plots, it is clear that all the poles for all the variants lie on the left half of the complex plane indicating stable transfer functions for which practical implementations are possible.

$$u \approx \frac{-0.03874s^4 - 0.3081s^3 + 5.36s^2 - 27.14s + 63.67}{s^5 + 7.031s^4 + 28.51s^3 + 70.47s^2 + 100.2s + 63.67} \tag{2.30}$$

$$t \approx \frac{0.1931s^4 - 2.265s^3 + 13.57s^2 - 46.62s + 85.97}{s^5 + 7.107s^4 + 30.61s^3 + 81.53s^2 + 125.3s + 85.97} \tag{2.31}$$

$$y \approx \frac{-0.0341s^4 - 0.2709s^3 + 5.019s^2 - 26.28s + 63.03}{s^5 + 7.129s^4 + 28.79s^3 + 70.65s^2 + 99.79s + 63.03} \tag{2.32}$$

$$\tau \approx \frac{0.1771s^4 - 2.151s^3 + 13.26s^2 - 46.58s + 87.15}{s^5 + 7.284s^4 + 31.46s^3 + 83.52s^2 + 127.7s + 87.15} \tag{2.33}$$

Figures 2.3 - 2.6 show Gaussian pulses with different values of σ and μ obtained

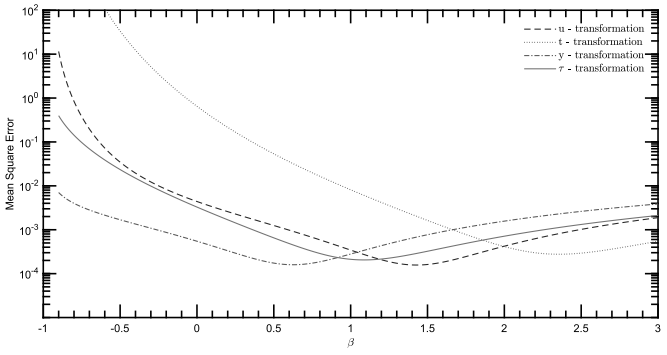

Figure 2.1: Variation of MSE with β for 5^{th} order approximation of the u, t, y and τ transformations for a Gaussian pulse ($\sigma = 0.5$, $\mu = 2$)

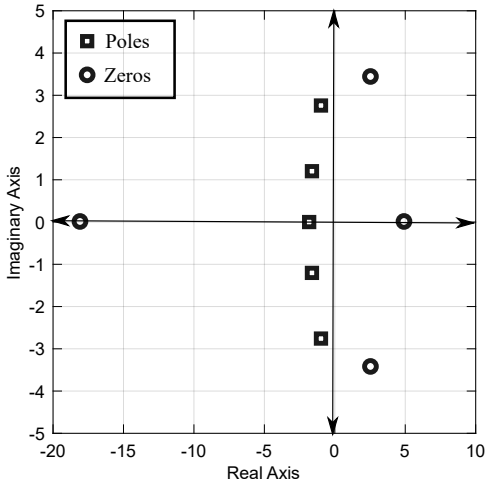

(a) Pole-Zero plot of Eq.(2.30)

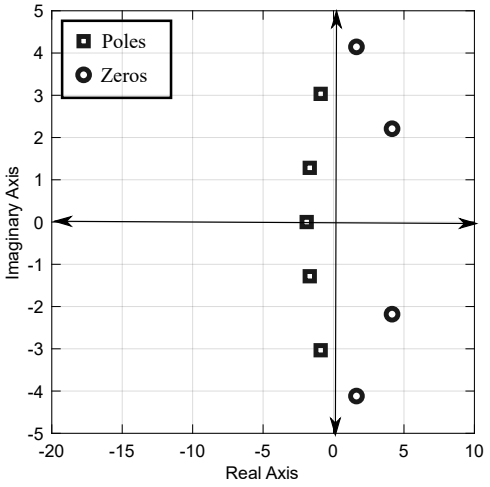

(b) Pole-Zero plot of Eq.(2.31)

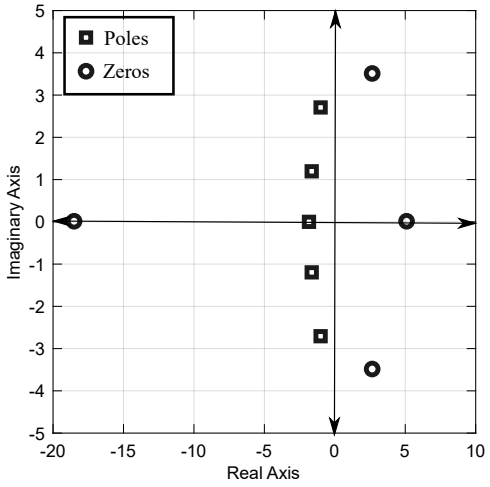

(c) Pole-Zero plot of Eq.(2.32)

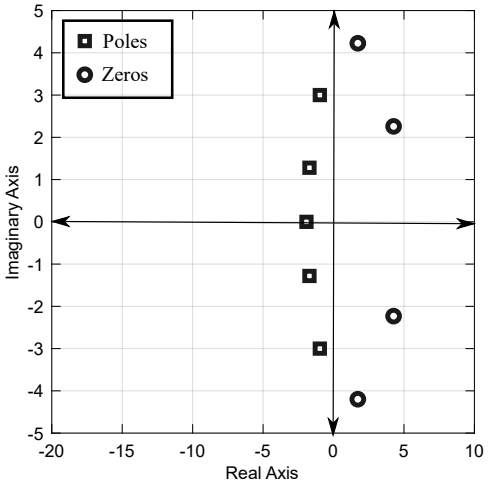

(d) Pole-Zero plot of Eq.(2.33)

Figure 2.2: Pole-Zero plots of the Gaussian transfer functions

using the u, t, y and τ-transformations respectively. From these figures, it is clear that all the four variants are able to obtain impulse responses close to the required pulse. If the time-shift parameter of the Gaussian pulse (μ) is high, then a higher order approximation might be required to be able to obtain an accurate impulse response.

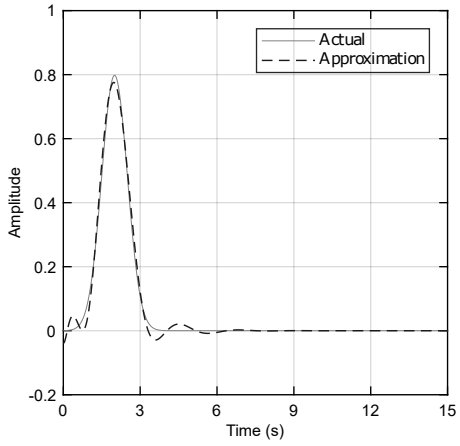

(a) $\sigma = 0.5$, $\mu = 2$, β=1.43, Order = 5

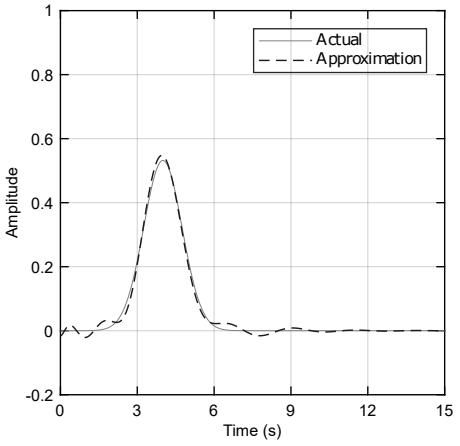

(b) $\sigma = 0.75$, $\mu = 4$, β=2.25, Order = 7

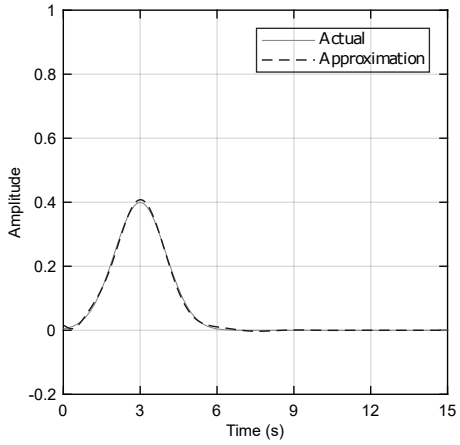

(c) $\sigma = 1$, $\mu = 3$, β=2.17, Order = 6

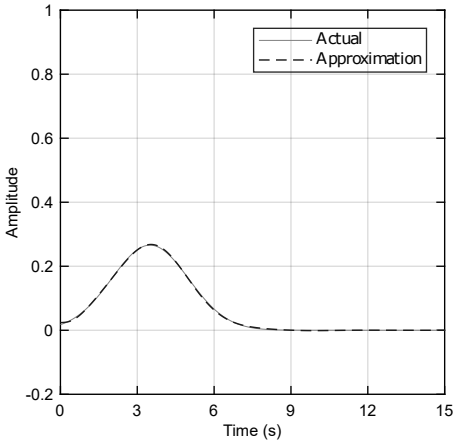

(d) $\sigma = 1.5$, $\mu = 3.5$, β=2.49, Order = 6

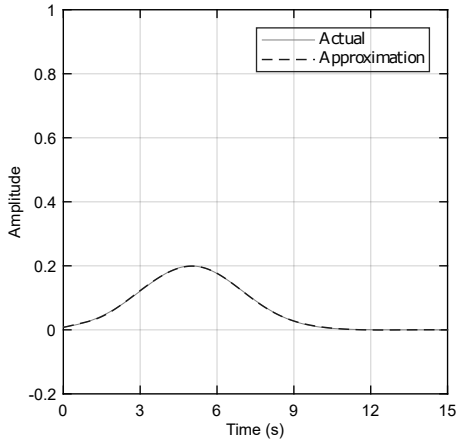

(e) $\sigma = 2$, $\mu = 5$, β=3.11, Order = 7

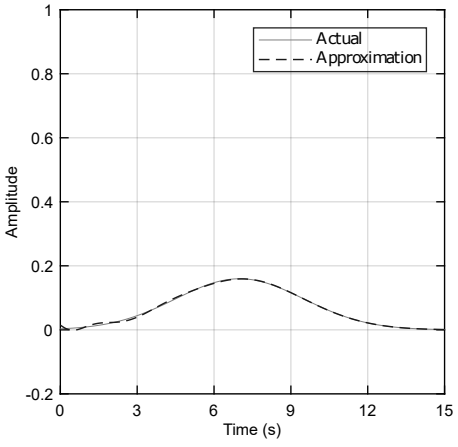

(f) $\sigma = 2.5$, $\mu = 7$, β=3.41, Order = 8

Figure 2.3: Gaussian impulse response approximation using u-transformation.

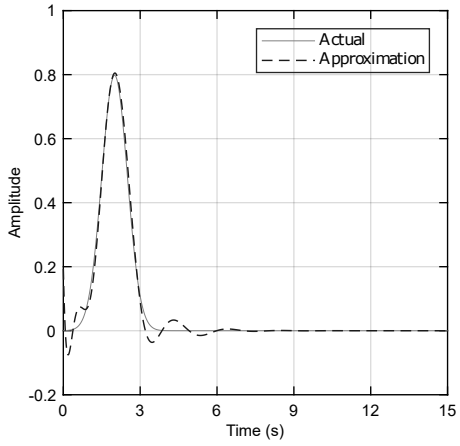

(a) $\sigma = 0.5$, $\mu = 2$, β=2.35, Order = 5

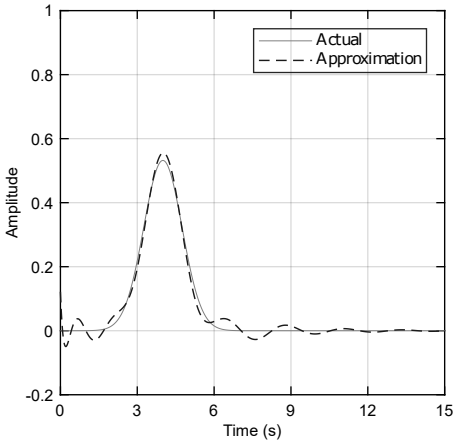

(b) $\sigma = 0.75$, $\mu = 4$, β=3.01, Order = 7

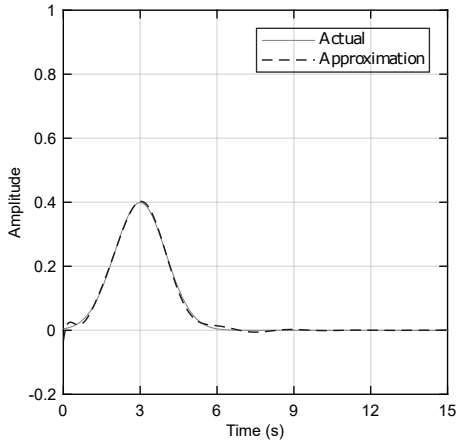

(c) $\sigma = 1$, $\mu = 3$, β=3.33, Order = 6

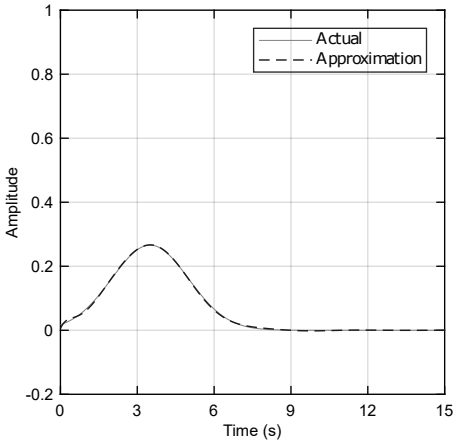

(d) $\sigma = 1.5$, $\mu = 3.5$, β=3.83, Order = 6

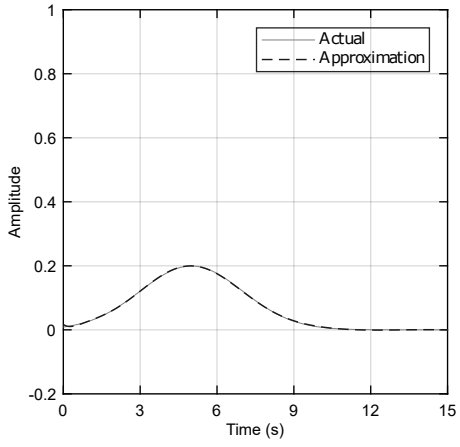

(e) $\sigma = 2$, $\mu = 5$, β=4.43, Order = 7

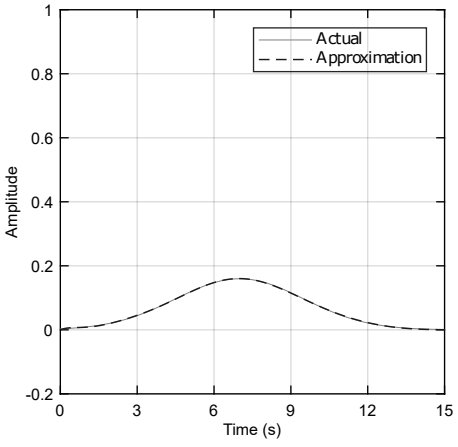

(f) $\sigma = 2.5$, $\mu = 7$, β=4.90, Order = 8

Figure 2.4: Gaussian impulse response approximation using t-transformation.

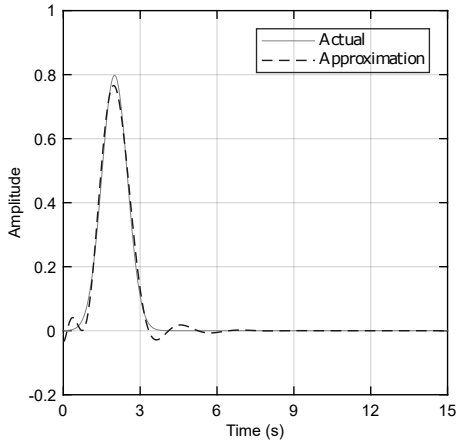

(a) $\sigma = 0.5$, $\mu = 2$, β=0.62, Order = 5

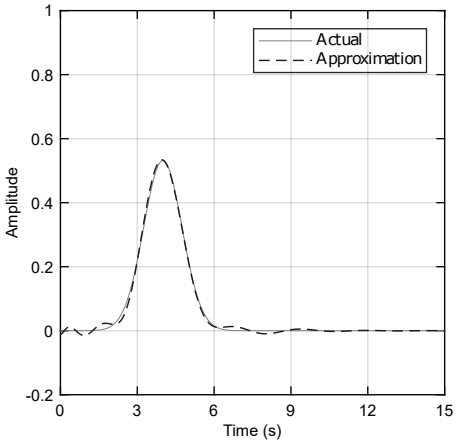

(b) $\sigma = 0.75$, $\mu = 4$, β=0.70, Order = 7

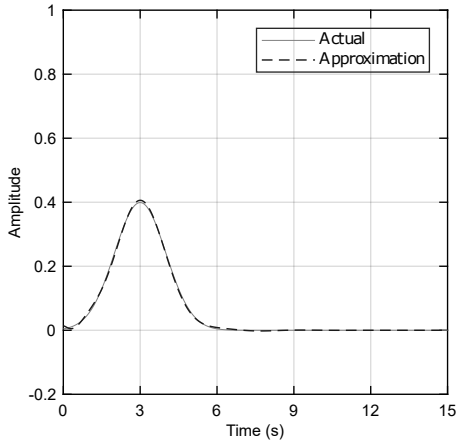

(c) $\sigma = 1$, $\mu = 3$, β=0.90, Order = 6

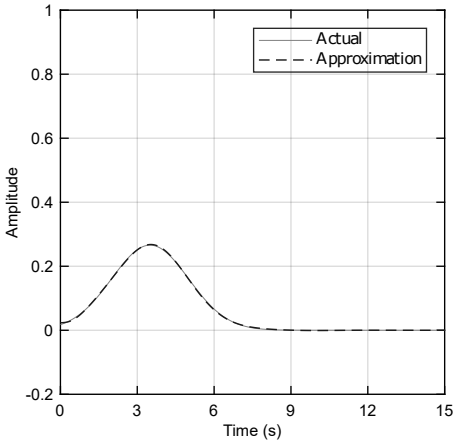

(d) $\sigma = 1.5$, $\mu = 3.5$, β=1.18, Order = 6

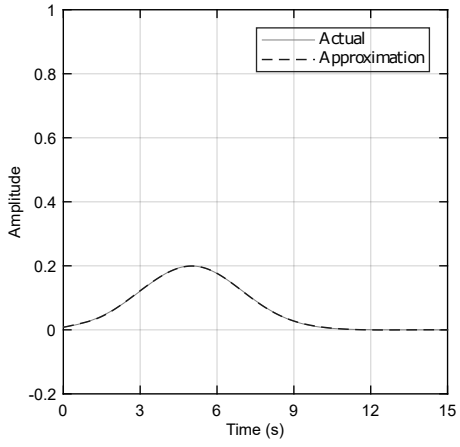

(e) $\sigma = 2$, $\mu = 5$, β=1.36, Order = 7

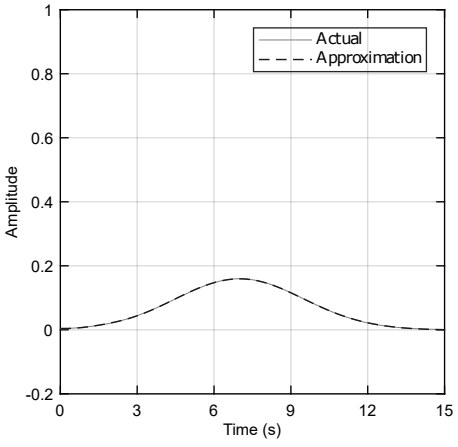

(f) $\sigma = 2.5$, $\mu = 7$, β=1.5, Order = 8

Figure 2.5: Gaussian impulse response approximation using y-transformation.

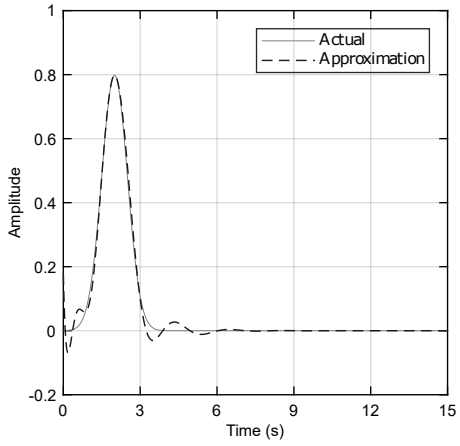

(a) $\sigma = 0.5$, $\mu = 2$, β=1.09, Order = 5

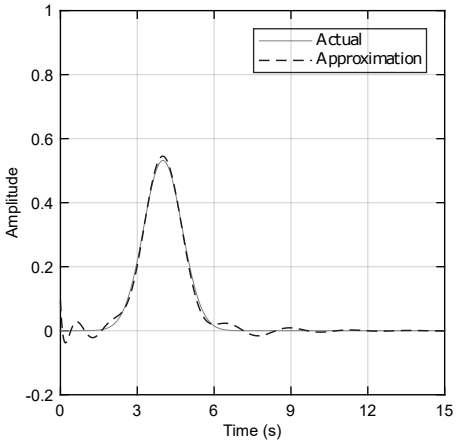

(b) $\sigma = 0.75$, $\mu = 4$, β=1.02, Order = 7

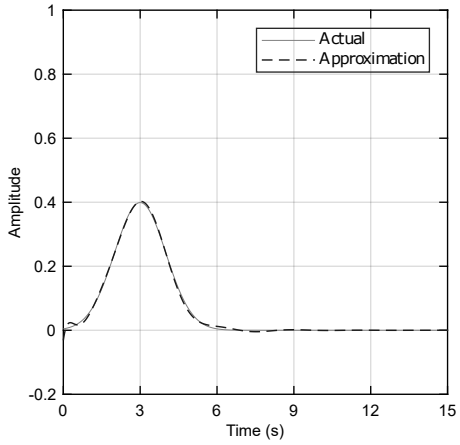

(c) $\sigma = 1$, $\mu = 3$, β=1.61, Order = 6

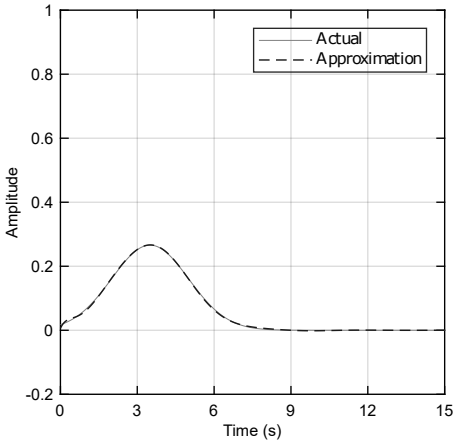

(d) $\sigma = 1.5$, $\mu = 3.5$, β=2.08, Order = 6

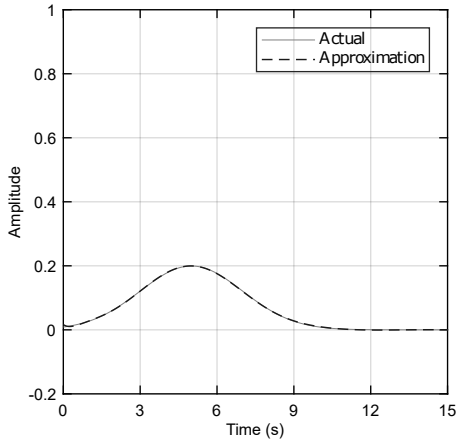

(e) $\sigma = 2$, $\mu = 5$, β=2.25, Order = 7

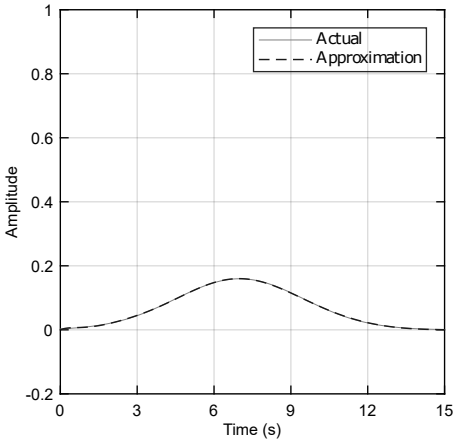

(f) $\sigma = 2.5$, $\mu = 7$, β=2.31, Order = 8

Figure 2.6: Gaussian impulse response approximation using τ-transformation.

2.5 Conclusion

In this chapter we studied the nonlinear sequence transformation technique as a potential method to convert a transfer function in the form of a power series to a rational function. There are several variants of nonlinear sequence transformation technique of which Levin and Weniger transformations have been used extensively in the literature. Levin's u and t-transformations and Weniger's y and τ-transformations have been used in this chapter to approximate Gaussian filters of different time-shift (μ) and scale (σ) parameters. A comparison among different variants and with other closed-form methods for a Gaussian filter was not done here because our aim has been to show that these variants can be used to successfully to arrive at a proper rational function.

Chapter 3

Approximation of Nonlinear Sequence Transformation-based Continuous-Time Wavelet Filter

As mentioned previously, continuous-time domain analog implementation of wavelet transforms is preferred over discrete-time when power consumption is a major constraint. It has been shown in [1, 22, 23, 35, 36, 68, 69] that Wavelet Transform (WT) implemented in continuous-time consumes extremely low power, of the order of pW, compared to discrete-time counterparts which consume power of the order of μW [70].

The WT, $W(\sigma, b)$, of a time varying signal $x(t)$ is given by

$$W(\sigma, b) = \frac{1}{\sqrt{\sigma}} \int_{-\infty}^{+\infty} x(t)\psi\left(\frac{t-b}{\sigma}\right) dt \tag{3.1}$$

where σ and b are the scaling and shifting parameters respectively and the function $\psi(t)$ is the mother wavelet.

It is known that the output response $y(t)$ of the signal $x(t)$ when passed through a Linear Time Invariant (LTI) system is the convolution of the signal with the impulse response $h(t)$ of the LTI system and is given by

$$y(t) = \int_{-\infty}^{\infty} x(t)h(\tau - t)dt \tag{3.2}$$

From (3.1) and (3.2) it can be established that WT of a signal can be computed by the convolution of the input signal $x(t)$ with a function whose impulse response is given by

$$h(t) = \frac{1}{\sqrt{\sigma}}\psi\left(\frac{-t}{\sigma}\right) \tag{3.3}$$

For practical implementations, the impulse response in (3.3) has to be causal which implies that $h(t)$ is zero for $t < 0$. Thus, wavelets are shifted by an acceptable value t_0 to meet this condition [71]. A wavelet function with a low value of t_0 can be approximated by a lower order system. However, this would result in truncation of energy as major portion of wavelet is in the region $t < 0$. Choosing a high value

for t_0 would result in zero truncation of energy but a higher order system is needed for approximation. Thus, an appropriate value for t_0 has to be chosen by trading-off truncation energy with order of approximation as was illustrated in [72]. Therefore, WT at a given scale can be obtained by implementing a filter with the transfer function

$$H(s) = \frac{1}{\sqrt{\sigma}} \int_{-\infty}^{\infty} \psi\left(\frac{t_0 - t}{\sigma}\right) e^{-st} dt \tag{3.4}$$

While $H(s)$ shown in (3.4) is of infinite dimension, from an implementation perspective, it needs to be finite dimensional and stable. Several techniques exist in the literature that yield rational and stable transfer functions. Accuracy of the impulse response of higher order approximations of these transfer functions is greater than lower order ones but the order of approximation is driven by practical constraints like power consumption, chip area, delay etc. Thus, a strictly proper rational approximation of $H(s)$ with real coefficients, preferably of lower order, needs to be obtained to be able to effectively compute the WT in analog domain.

Approximation methods described in [27, 46, 73] synthesize wavelet filter transfer functions but are limited to wavelet bases related to Gaussian function. A more generic procedure known as Padé approximation, which is based on Taylor series, has been used in [74]. Several types of wavelets including complex wavelets have been approximated using this technique [75–77].

A generic approximation procedure that reduces the L_2 norm between an approximation and actual wavelet by numerical optimization, called L_2 method, has been proposed in [71]. Solutions obtained by this method rely on local search routines and also there is a risk of ending up at local optima. The final outcome of this method depends largely on the starting points. Different starting points result in different solutions after optimization and a good starting point may avoid local optima. An automated methodology which generates starting points for L_2 method has been devised in [1]. Yet another optimization method that minimizes the weighted square error between an approximation and actual wavelet has been proposed in [25].

In this chapter, proper rational approximation of wavelet transfer functions is attempted initially using two major variants of nonlinear sequence transformation, namely Levin's transformations and Weniger's transformations [47] discussed in Chapter 2. However, these variants do not obtain Bounded Input Bounded Output (BIBO) stable rational functions when applied to wavelets due to irregularities in leading terms of the Taylor series of the wavelet function. Thus, in this Chapter we propose certain other variants of nonlinear sequence transformation that obtain proper rational approximation for wavelets by avoiding irregular Taylor coefficients.

3.1 Nonlinear Sequence Transformation and Problem with leading irregular Taylor coefficients

A common term in the remainder estimate ω_n of the four variants (Levin's u and t, Weniger's y and τ) is ΔS_{n-1}. This term determines two important parameters of these four variants for a given value of k:

(i) The order of approximation given as $\frac{k+n-1}{k}$ and

(ii) The Taylor coefficients used in construction of denominator polynomial given as a_{n-1} to a_{k+n-1}.

To obtain proper rational approximations using these transformations, the parameter n in equation (2.13) should be taken as 1. However, this choice of $n = 1$ leads to rational approximations which are not BIBO stable. The instability problem is highlighted with the help of Table 3.1, which contains pole-zero information of 5^{th} order approximations ($k = 5$) of Gaussian Wavelet (first derivative of Gaussian function) and Mexican Hat wavelet (second derivative of Gaussian function). It is clear that some of the poles (highlighted in bold) of rational approximation obtained by each variant crossed over to the right half plane, which will lead to instability [78].

Nonlinear sequence transformation makes use of regularities in the elements of sequence (which in this case are Taylor coefficients of Laplace transforms of wavelet functions) to be transformed. In some cases, the leading terms of elements of a sequence behave irregularly (that is, certain leading terms grow in magnitude like the terms

Table 3.1: Zeros and Poles of 5^{th} order Approximations of Gaussian wavelet and Mexican Hat wavelet Obtained by different variants of Nonlinear sequence transformation

	Guassian Wavelet $(t_0 = 2, \sigma = 1)$ $\psi(t) = -\mathrm{e}^{-(t-2)^2}\,(2\,t-4)$		Mexican Hat Wavelet $(t_0 = 2, \sigma = 1)$ $\psi(t) = \mathrm{e}^{-(t-2)^2}\,(2\,t-4)^2 - 2\,\mathrm{e}^{-(t-2)^2}$	
	Zeros	Poles	Zeros	Poles
u	$1.9026 \pm 3.2783i$	$\mathbf{0.7653 \pm 1.4057i}$	-0.8091	$\mathbf{0.2489 \pm 0.4200i}$
	-7.6031	$-0.5627 \pm 0.7556i$	0.8827	$-0.2841 \pm 0.2165i$
	0.0106	-0.8195	$0.2978, -0.1706$	**167**
t	$1.2297 \pm 2.9736i$	$\mathbf{0.9695 \pm 2.2582i}$	-1.8290	$\mathbf{0.3190 \pm 0.5691i}$
	4.7414	$-0.8305 \pm 0.9916i$	1.4022	$-0.3717 \pm 0.2762i$
	0.0106	-1.1066	$0.2818, -0.1686$	**320.11**
y	$1.0333 \pm 3.1133i$	$\mathbf{0.6404 \pm 0.9540i}$	-0.5612	$\mathbf{0.2161 \pm 0.3473i}$
	-4.7625	$-0.4149 \pm 0.6196i$	0.5642	$-0.2423 \pm 0.1885i$
	0.0106	-0.6581	$0.3667, -0.1737$	**80.0524**
τ	$1.1807 \pm 3.1175i$	$\mathbf{0.7462 \pm 1.1485i}$	-0.8205	$\mathbf{0.2488 \pm 0.4057i}$
	$-2.8163e02$	$-0.4936 \pm 0.7173i$	0.8061	$-0.2802 \pm 0.2164i$
	0.0106	-0.7642	$0.3010, -0.1707$	**100**

of a mildly divergent series) resulting in approximations which make no sense as described in [79]. Therefore, the instability observed in approximating wavelet transfer functions in Table 3.1 can be attributed to the presence of leading irregular Taylor coefficients. This irregularity is better understood by varying the translation parameter of a wavelet function as shown in figure 3.1, where the absolute percentage change in Taylor coefficients (a_0 to a_5) of a Gaussian wavelet is shown as the translation parameter is varied. It is evident from this figure that the behaviour of the leading term a_0 is irregular as compared to other coefficients a_1 to a_5.

As discussed earlier, the Taylor coefficients a_{n-1} to a_{k+n-1} are used to construct the k^{th} order denominator polynomial using four variants of nonlinear sequence transformation. Now, considering the Gaussian wavelet and taking the index n to be 2, will

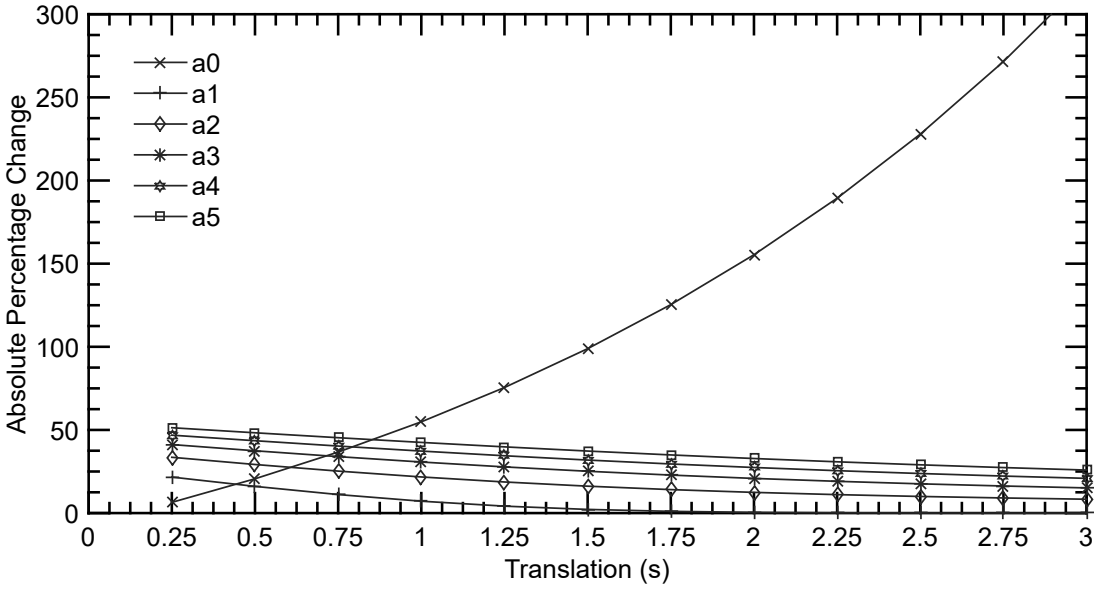

Figure 3.1: Absolute percentage change of Taylor Coefficients $a_0 - a_5$ of Gaussian wavelet as the translation is increased

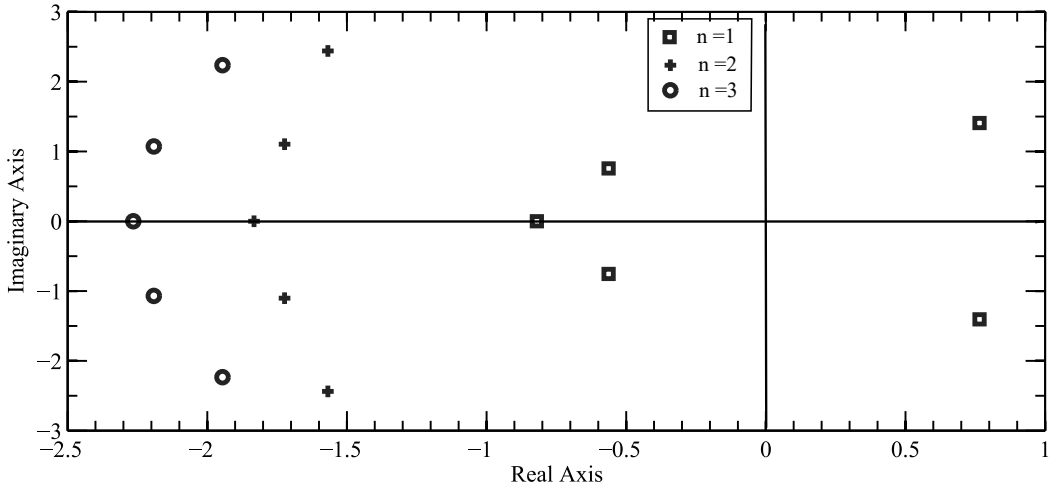

Figure 3.2: Location of Poles on the complex plane as n is varied for a 5^{th} order u-transformation approximation of Gaussian wavelet ($t_0 = 2$, $\sigma = 1$)

result in the Taylor coefficients $a_1, a_2, \cdots a_{k+1}$ being used, thereby avoiding a_0 which has been shown to be irregular. Figure 3.2 shows the location of the roots of the denominator polynomial of the 5^{th} order u-transformation approximation of Gaussian wavelet ($t_0 = 2$, $\sigma = 1$) as the value of the index n is varied. It is clear that for n greater than 1, all the roots are on the left half of the complex plane, indicating a Hurwitz denominator polynomial [78], as opposed to the case when $n = 1$ where some of the roots crossed over to the right half. But a choice of $n > 1$ gives rise to improper rational approximations since the order of approximation varies with n as $\frac{k+n-1}{k}$ as mentioned earlier. Such improper rational functions, as is known, are not suitable for practical implementation.

3.2 Proposed Variants to Obtain Proper Rational Approximations for Wavelets with Leading Irregular Taylor Coefficients

The proposed variants make use of the fact that a polynomial of the order $k-1$, described by equation (2.12), is also completely annihilated by a forward difference operator of the order $k+p$ (Δ^{k+p}), where p is a positive integer. That is,

$$\Delta^{k+p}\left(\frac{S_n - S}{\omega_n}(n+\beta)^{k-1}\right) = \Delta^{k+p}\big(P_{k-1}(n)\big) \tag{3.5}$$

The RHS of equation (3.5) is a polynomial of the order $k-1$ which is annihilated completely by applying Δ^{k+p}. Since the application of Δ^{k+p} leads to approximations of the order $k+p$ conforming to equation (2.14), the limits of Δ^{k+p} in the proposed variants are truncated to k to obtain a k^{th} order approximation. However, truncation of the limits of summation to k does not lead to complete annihilation of the RHS of equation (3.5) resulting in a truncation error (T_e) as shown in equation (3.6)

$$T_e = -\sum_{j=k+1}^{k+p} (-1)^j \binom{k+p}{j} P_{k-1}(n+j) \tag{3.6}$$

This truncation error T_e is ignored for the variants being proposed in this work and consequences of the same are discussed below:

Rearranging the terms of equation (3.5) ignoring the truncation error T_e, we obtain

$$S \approx \frac{\sum_{j=0}^{k} (-1)^j \binom{k+p}{j} (n+k+p-j+\beta)^{k-1} \frac{S_{n+k+p-j}}{\omega_{n+k+p-j}}}{\sum_{j=0}^{k} (-1)^j \binom{k+p}{j} (n+k+p-j+\beta)^{k-1} \frac{1}{\omega_{n+k+p-j}}} \tag{3.7}$$

The limits of the term representing the Taylor coefficients S_{n+k+p} in equation (3.7) are also truncated to k which results in,

$$S_{n+k+p} \approx \sum_{i=0}^{n+k-1} a_i s^i \tag{3.8}$$

where S_{n+k+p} is a function of s and a_i is the i^{th} Taylor coefficient. Now, a variant

similar to Levin u-transformation is obtained by substituting $\omega_n = (n+\beta)\Delta S_{n-1}$ and equation (3.8) in equation (3.7). We designate it as $\widehat{u}$-transformation shown below:

$$\widehat{u} \approx \frac{\sum_{j=0}^{k} \frac{(-1)^j \binom{k+p}{j} (1+k+p-j+\beta)^{k-2}}{a_{k+p-j} s^{k+p-j}} \sum_{i=0}^{k-j} a_i s^i}{\sum_{j=0}^{k} \frac{(-1)^j \binom{k+p}{j} (1+k+p-j+\beta)^{k-2}}{a_{k+p-j} s^{k+p-j}}} \tag{3.9}$$

In obtaining the above equation, the expression $\Delta S_{n+j-1} = a_{n+j-1} s^{n+j-1}$ has been used. The minimal index of the Taylor coefficients to be used in the approximation, n, is taken as 1 so as to obtain proper rational approximation.

By changing the index of summations of the numerator in equation (3.9) using the identity $\sum_{j=0}^{k} a_j = \sum_{j=0}^{k} a_{k-j}$, we obtain

$$\widehat{u} \approx \frac{\sum_{j=0}^{k} \frac{(-1)^{k-j} \binom{k+p}{k-j} (1+p+j+\beta)^{k-2}}{a_{p+j} s^{p+j}} \sum_{i=0}^{j} a_i s^i}{\sum_{j=0}^{k} \frac{(-1)^j \binom{k+p}{j} (1+k+p-j+\beta)^{k-2}}{a_{k+p-j} s^{k+p-j}}} \tag{3.10}$$

By changing the limits of the double finite summation present in the numerator of equation (3.10) using the identity $\sum_{j=0}^{k} \sum_{i=0}^{j} a_{j,i} = \sum_{i=0}^{k} \sum_{j=i}^{k} a_{j,i}$ and changing the index of the numerator summation involving j again, we obtain

$$\widehat{u} \approx \frac{\sum_{i=0}^{k} s^j \sum_{j=i}^{k} (-1)^{j-i} \binom{k+p}{j-i} (1+k+p-j+i+\beta)^{k-2} \frac{a_i}{a_{k+p-j+i}}}{\sum_{j=0}^{k} s^j (-1)^j \binom{k+p}{j} (1+k+p-j+\beta)^{k-2} \frac{1}{a_{k+p-j}}} \tag{3.11}$$

Rearranging the limits of double summation once again as well as changing the index

of the numerator summation involving i in the above equation, we obtain the final expression for the proposed $\widehat{u}$-transformation as

$$\widehat{u} \approx \frac{\sum_{j=0}^{k} s^j \sum_{i=0}^{j} (-1)^i \binom{k+p}{i} (1+k+p-i+\beta)^{k-2} \frac{a_{j-i}}{a_{k+p-i}}}{\sum_{j=0}^{k} s^j (-1)^j \binom{k+p}{j} (1+k+p-j+\beta)^{k-2} \frac{1}{a_{k+p-j}}} \tag{3.12}$$

From the denominator polynomial in the above equation, it is clear that the Taylor coefficients a_p to a_{k+p} are used in the approximation of the denominator polynomial, thereby eliminating the use of first p terms a_0 to a_{p-1}.

Now, choosing the remainder estimate to be $\omega_n = \Delta S_{n-1}$ and following the procedure mentioned through the equations (3.9)-(3.12), a transformation similar to Levin's t-transformation, which we name as $\widehat{t}$-transformation, is obtained as given in the following equation:

$$\widehat{t} \approx \frac{\sum_{j=0}^{k} s^j \sum_{i=0}^{j} (-1)^i \binom{k+p}{i} (1+k+p-i+\beta)^{k-1} \frac{a_{j-i}}{a_{k+p-i}}}{\sum_{j=0}^{k} s^j (-1)^j \binom{k+p}{j} (1+k+p-j+\beta)^{k-1} \frac{1}{a_{k+p-j}}} \tag{3.13}$$

The powers $(1+\beta)^k$ in equations (3.12) and (3.13) replaced by Pochhammer symbols $(1+\beta)_k$ result in the proposed approximations $\widehat{y}$ (3.14) and $\widehat{\tau}$ transformations (3.15)

similar to Weniger y and τ transformations:

$$\widehat{y} \approx \frac{\sum_{j=0}^{k} s^j \sum_{i=0}^{j} (-1)^i \binom{k+p}{i} (1+k+p-i+\beta)_{k-2} \frac{a_{j-i}}{a_{k+p-i}}}{\sum_{j=0}^{k} s^j (-1)^j \binom{k+p}{j} (1+k+p-j+\beta)_{k-2} \frac{1}{a_{k+p-j}}} \tag{3.14}$$

$$\widehat{\tau} \approx \frac{\sum_{j=0}^{k} s^j \sum_{i=0}^{j} (-1)^i \binom{k+p}{i} (1+k+p-i+\beta)_{k-1} \frac{a_{j-i}}{a_{k+p-i}}}{\sum_{j=0}^{k} s^j (-1)^j \binom{k+p}{j} (1+k+p-j+\beta)_{k-1} \frac{1}{a_{k+p-j}}} \tag{3.15}$$

From the equations (3.12)-(3.15), it is clear that the number of Taylor coefficients computed are $k+p+1$ (a_0 to a_{k+p}). While all the coefficients a_0 to a_{k+p} are used for computing the numerator polynomial, the coefficients a_p to a_{k+p} only are used for computing the denominator polynomial.

3.2.1 Choice of the parameters p and β

In the proposed variants given in equations (3.12) - (3.15), the parameter p helps in avoiding the leading Taylor coefficients. Given a Taylor series, it is therefore important to compute a value for p. A method to do this is given in Lemma 1 below:

Lemma 1:The $k+1$ Taylor coefficients a_p, a_{p+1},$\cdots$,a_{k+p} used in construction of the k^{th} order denominator polynomial in equations (3.12) - (3.15) have to satisfy the inequality

given by,

$$a_{p+l} \cdot a_{p+l+1} < 0 \; \forall \; l \; (l = 0 \; to \; k-1) \tag{3.16}$$

Proof: Necessary condition for the BIBO stability [78] of a rational function mandates that all the coefficients of the denominator polynomial exist and have the same sign. From the proposed transformations (3.12) - (3.15), it is clear that each coefficient of the denominator polynomial is multiplied by $(-1)^{k+p-j}$ which results in a polynomial with alternating signs. Hence the $k+1$ Taylor coefficients a_p to a_{k+p} have to be strictly alternating proving the inequality given by equation (3.16). Hence, the leading p terms that do not follow the equation (3.16) should be avoided. The value of p need not always be the least value which satisfies the equation (3.16) but can also be of higher value.

Once a value for p is finalized from Lemma 1, a minimum value for β can be chosen from the following inequality.

$$\beta \; > \; -(p+1) \tag{3.17}$$

This is obtained from the fact that the factor $(1+k+p-j+\beta)$ in equations (3.12) - (3.15) should always be positive. The process of choosing an exact value of β during the approximation is detailed in the next Section.

3.2.2 Rational approximation and admissibility property

An important property of the wavelet transform is that the wavelet $\psi(t)$ should have at least one vanishing moment. This is known as the wavelet admissibility condition [31] and is given by

$$\int_{-\infty}^{\infty} \psi(t)dt = 0 \tag{3.18}$$

It is known that the impulse response $h(t)$ of the wavelet filter obtained from the approximated transfer function $H(s)$ (equation 3.4) should also satisfy the admissibility property. In the Laplace domain this requirement translates to having a zero component at zero frequency i.e, $H(0) = 0$.

The admissibility property would be satisfied by the proposed approximations (3.12) - (3.15), if the first Taylor coefficient of $H(s)$, a_0 is allowed to be zero. Alternatively, this property would be satisfied if the constant term of the numerator is allowed to be zero after the approximation is made. The latter approach is followed in this work since the term a_0 plays a role in determining all the coefficients of the numerator polynomial.

3.3 Approximation of Different Wavelet Bases using Proposed Variants

In this section we demonstrate how the proposed variants can be used to approximate different wavelet bases. First, a wavelet at a given dilation (σ) and translation (t_0) is chosen, then its Laplace transform is computed and the corresponding Taylor series expansion around zero is obtained. For a given order of approximation k, the value of p (the number of leading irregular Taylor coefficients to be avoided) is selected with the help of Lemma1 mentioned earlier. A minimum value of β for a given value of p is then obtained from the equation (3.17). As the value of β is varied around the minimum value, the impulse response also varies which is different for different variants proposed. Each variant has it's own value of β for which the impulse response obtained has a minimum mean square error (MSE) with reference to the actual wavelet. Figure 3.3 shows the variation of mean square error of the 5^{th} order approximation of the Gaussian wavelet as β is varied.

Referring to the parameter n mentioned earlier, a value greater than the number of leading irregular Taylor coefficients results in a Hurwitz polynomial in the denominator (all poles lying on the left half of the complex plane) as can be seen from figure 3.2. Similarly, the value of p greater than the value obtained by the least value satisfying Lemma 1 for a given value of k, also successfully avoids the leading irregular Taylor

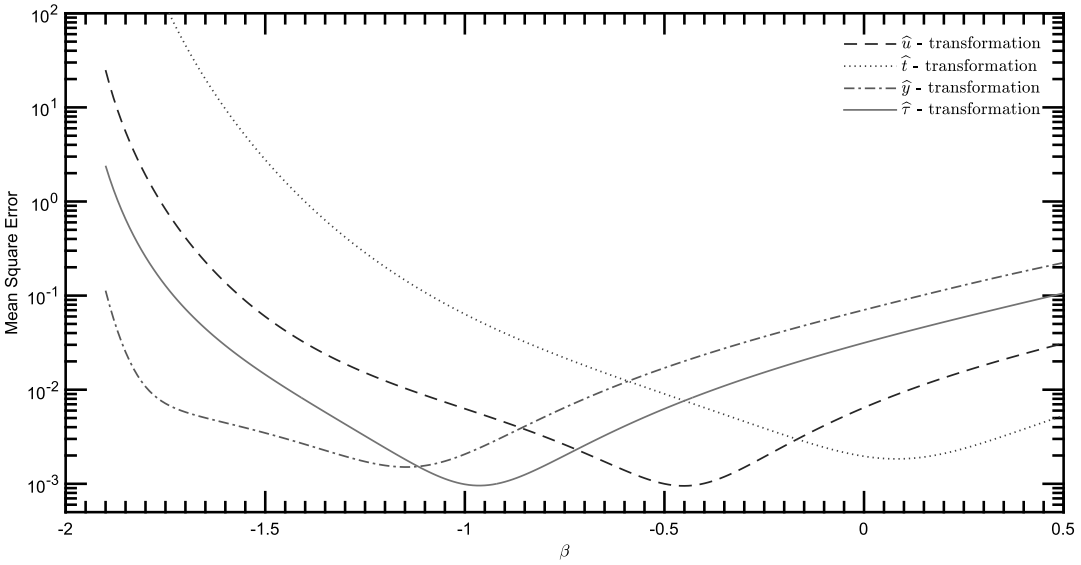

Figure 3.3: Variation of MSE with β for 5^{th} order approximation of the proposed variants (p=1) for a Gaussian wavelet ($t_0 = 2$, $\sigma = 1$)

coefficients. Tables 3.2-3.5 show the variation of MSE for a given order as p is increased for the proposed $\widehat{u}$, $\widehat{t}$, $\widehat{y}$ and $\widehat{\tau}$- approximations of Gaussian wavelet respectively.

Table 3.2: Variation of minimum MSE as p is varied for $\widehat{u}$-transformation approximation of Gaussian wavelet. (the corresponding β value for which the mininum MSE occurs is given in braces)

	order 4	order 5	order 6	order 7
p=1	**0.0095** (-0.88)	**9.50e-4** (-0.45)	5.99e-4 (-0.1)	3.69e-4 (0.27)
p=2	0.0114 (-1.65)	0.0019 (-1.18)	**2.41e-4 (-0.74)**	2.15e-5 (-0.43)
p=3	0.0126 (-2.57)	0.0027 (-2.05)	2.90e-4 (-1.57)	**1.97e-4** (-1.25)
p=4	0.0136 (-3.56)	0.0035 (-2.98)	3.77e-4 (-2.50)	2.02e-4 (-2.17)

Once the values of p and β are finalized, the important property of admissibility is ensured by making the constant term of the numerator polynomial, if any, to zero. If strictly proper rational approximations are required then the numerator polynomials in (3.12) - (3.15) are truncated to $k-1$.

Table 3.3: Variation of minimum MSE as p is varied for $\widehat{t}$-transformation approximation of Gaussian wavelet. (the corresponding β value for which the mininum MSE occurs is given in braces)

	order 4	order 5	order 6	order 7
p=1	**0.0031** (-0.30)	0.0018 (0.08)	0.0017 (0.49)	7.38e-4 (1.17)
p=2	0.0051 (-0.98)	**8.51e-4 (-0.58)**	7.44e-4 (-0.20)	3.06e-4 (0.3)
p=3	0.0066 (-1.81)	8.81e-4 (-1.44)	4.68e-4 (-1.09)	**2.28e-4** (-0.71)
p=4	0.0078 (-2.74)	0.0010 (-2.39)	**3.91e-4 (-2.03)**	2.55e-4 (-1.71)

Table 3.4: Variation of minimum MSE as p is varied for $\widehat{y}$-transformation approximation of Gaussian wavelet. (the corresponding β value for which the mininum MSE occurs is given in braces)

	order 4	order 5	order 6	order 7
p=1	**0.0103** (-1.23)	**0.0015 (-1.15)**	**1.19e-4 (-1.14)**	6.88e-4 (-1.19)
p=2	0.0120 (-2.02)	0.0026 (-1.89)	2.01e-4 (-1.84)	3.14e-5 (-1.88)
p=3	0.0131 (-2.94)	0.0035 (-3.69)	3.45e-4 (-2.70)	**2.90e-5** (-2.71)
p=4	0.0141 (-3.93)	0.0013 (-3.53)	3.72e-4 (-3.61)	4.32e-5 (-3.61)

Table 3.5: Variation of minimum MSE as p is varied for $\widehat{\tau}$-transformation approximation of Gaussian wavelet. (the corresponding β value for which the mininum MSE occurs is given in braces)

	order 4	order 5	order 6	order 7
p=1	**0.0038** (-1.02)	**6.69e-4** (-1.03)	4.83e-4 (-1.01)	1.99e-4 (-0.84)
p=2	0.0059 (-1.71)	6.84e-4 (-1.72)	1.89e-4 (-1.74)	8.24e-5 (-1.68)
p=3	0.0073 (-2.56)	9.69e-4 (-2.59)	**1.16e-4** (-2.60)	**4.61e-5** (-2.65)
p=4	0.0085 (-3.50)	0.0013 (-3.53)	1.39e-4 (-3.51)	5.06e-5 (-3.59)

A 5^{th} order approximation of the Gaussian wavelet, for example, obtained with the proposed $\widehat{\tau}$-approximation that has minimum MSE of all the proposed variants, for $p = 1$ and $\beta = -1.03$, is given by equation (3.19) and is shown in figure 3.4(a).

$$\frac{-0.0061s^4 + 2.985s^3 - 8.996s^2 + 51.63s}{s^5 + 6.042s^4 + 21.21s^3 + 45.2s^2 + 55.07s + 29.77} \tag{3.19}$$

This method can also be used to approximate several mother wavelet bases. Figure

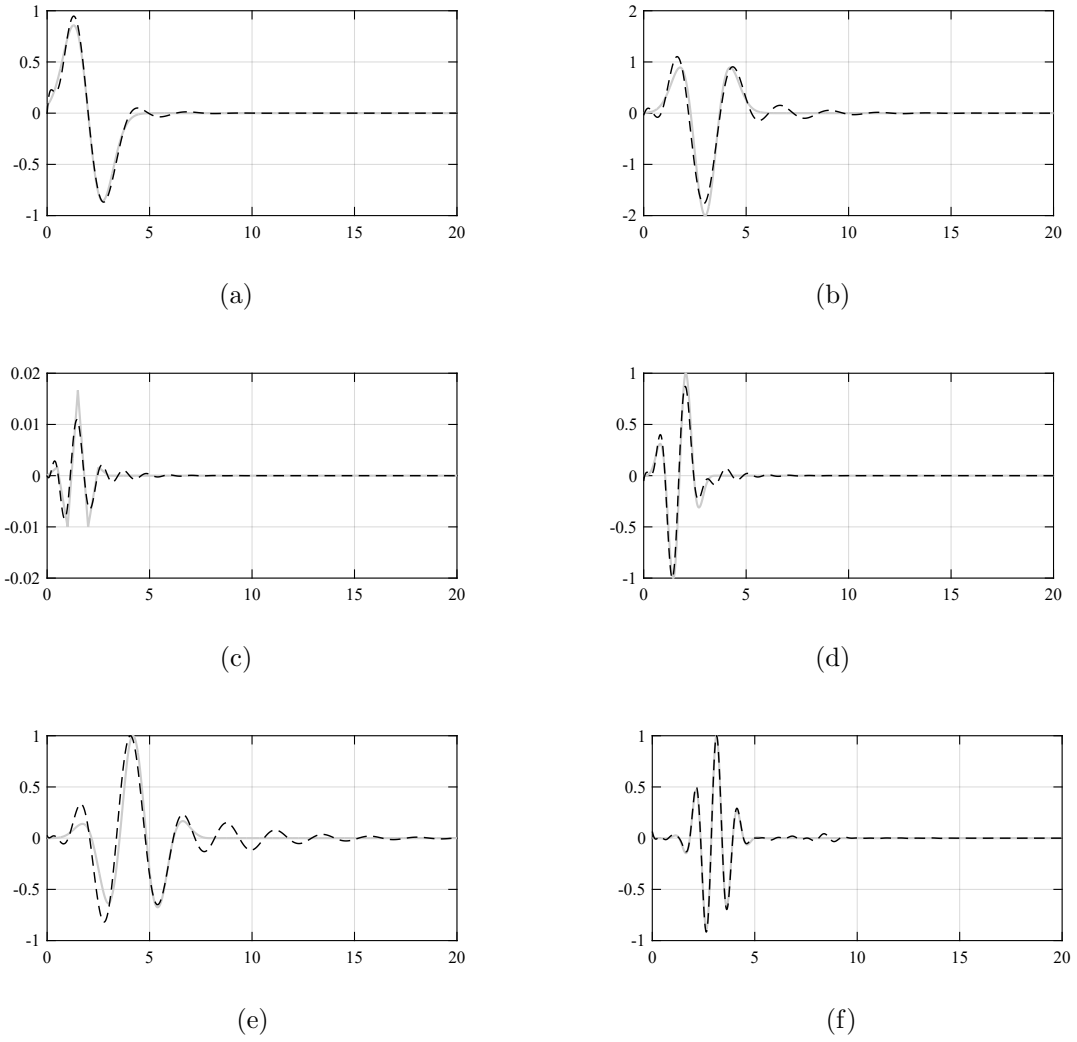

Figure 3.4: Wavelet base approximations carried out using the proposed variants. The thick gray line is the wavelet and the dashed black line is the impulse response of the approximated wavelet. Following wavelets are approximated with orders $O()$ and time shifts $T()$: (the scale σ is 1 unless specified otherwise) (a) Gaussian Wavelet $O(5), T(2)$ (b) Mexican Hat Wavelet $O(7)$,$T(3)$ (c) Compactly supported Spline Wavelet of order 2 O(8) T(0) (d) 3^{rd} derivative of B-Spline of order 7, $O(9), T(0)$, $\sigma = 0.5$ (e) 4^{th} derivative of Exponential-Spline of order 8, $\alpha = 0.25$, $O(9), T(0)$ (f) Morlet Wavelet (Gaussian multiplied by cosine of angular frequency $6rad/sec$),$O(10), T(3)$.

3.4 shows approximations of wavelet bases such as Gaussian wavelet, Morlet wavelet and Mexican Hat wavelets. Wavelets belonging to the spline wavelet family like interpolatory splines [80], compactly supported splines [81], exponential splines [82] have also been approximated using the proposed method and the same are shown in figure 3.4.

The Table 3.6 illustrates the trade-off between truncation of energy and approximation complexity for the proposed $\widehat{\tau}$-transformation while approximating a Gaussian wavelet. Such kind of tabulation helps in choosing an appropriate value for t_0 before proceeding for implementation.

Table 3.6: Effect of the time shift on the Order of approximation, MSE and Energy Loss for the $\widehat{\tau}$-transformation when approximating Gaussian wavelet (σ =1)

	shift 2.0	shift 2.5	shift 3.0	shift 3.5
Order	MSE			
4	0.0038	0.0103	0.0188	0.0273
5	6.69e-4	0.0019	0.0053	0.0109
6	1.16e-4	4.54e-4	0.0014	0.0038
7	4.61e-5	1.23e-4	3.28e-4	9.26e-4
8	1.33e-5	5.26e-5	1.38e-4	3.02e-4
9	2.09e-6	1.51e-5	5.77e-5	1.53e-4
Energy Loss	7.10e-4	9.67e-6	4.73e-8	3.15e-10

3.4 Performance Evaluation

3.4.1 Comparison with Padé Method

The mean square error between the impulse responses obtained and the actual wavelets is used as a measure of comparison between different approximation methods. Since the proposed variants result in closed-form solutions, comparison is first made with the Padé method. As discussed in [79], the variant of nonlinear sequence transformation that gives the best MSE has not yet been established. It depends on the sequence to be transformed and any one of the variants gives the best MSE for a given order. This behaviour can be observed for the variants proposed in this work, as seen from figure 3.5, which shows the MSE plotted against different orders of approximations for different wavelets.

In case of the Gaussian wavelet, the proposed $\widehat{\tau}$-transformation performs better than the Padé method for all the orders as seen from figure 3.5(a). Among other variants, while the $\widehat{t}$-transformation performs the best for the orders 4 and 5, the $\widehat{y}$-transformation performs the best for the orders 6 through 8. In case of the Mexican Hat wavelet, the $\widehat{\tau}$-transformation performs as well as or better than the Padé method for all orders as seen from figure 3.5(b). While the $\widehat{t}$-transformation performs the best for orders 6 and 7, the $\widehat{\tau}$-transformation gives the best MSE for orders 8 through 10. The 9^{th} order $\widehat{\tau}$-transformation can be clearly seen to be performing on par with

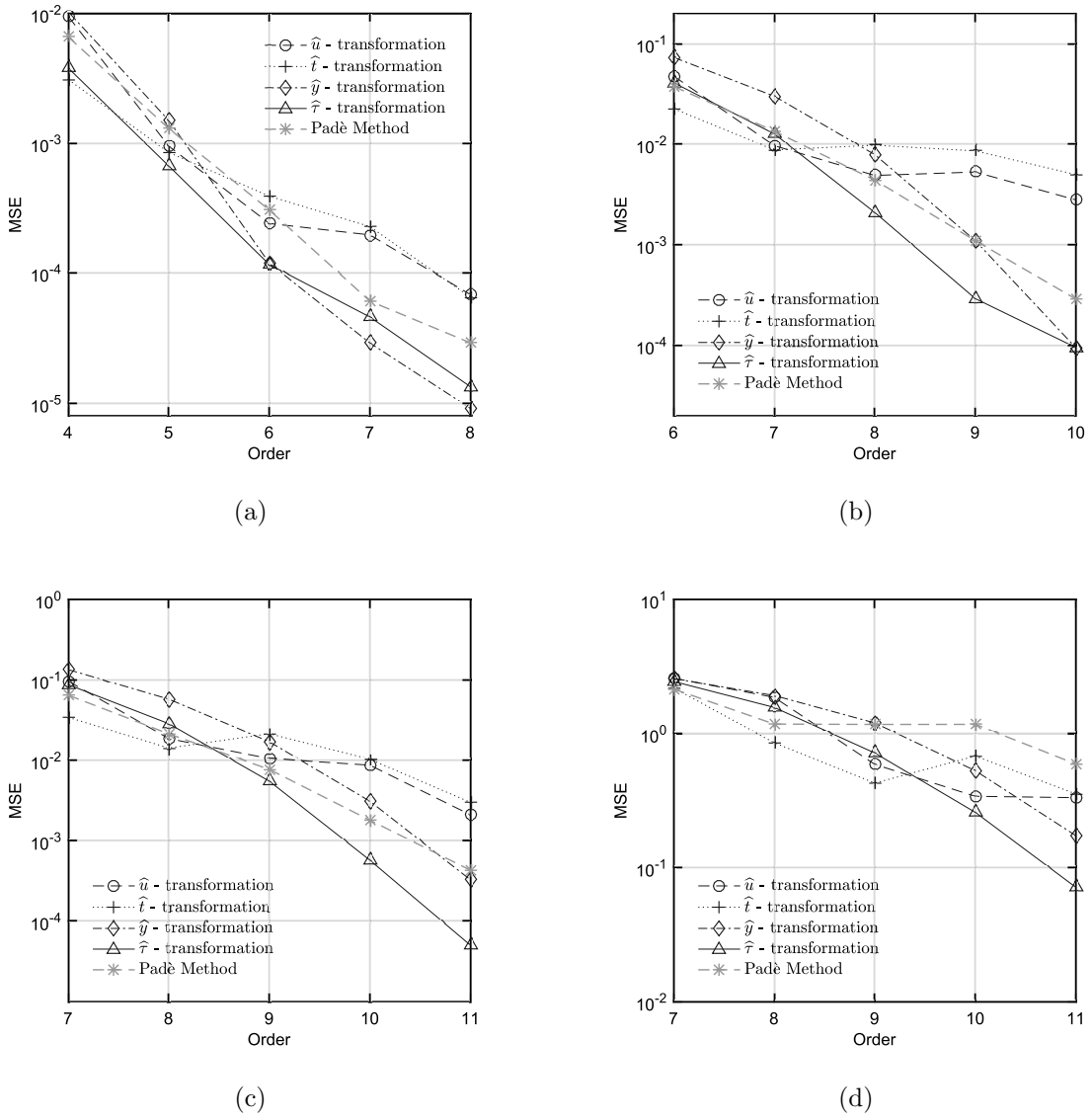

Figure 3.5: MSE versus order of approximation for Padé and Proposed variants for (a) Gaussian Wavelet ($t_0 = 2, \sigma = 1$) (b) Mexican Hat Wavelet ($t_0 = 3, \sigma = 1$) (c) Third derivative of seventh order B-spline ($t_0 = 0, \sigma = 0.5$) (d) Fourth derivative of eighth order Exponential spline ($t_0 = 0, \sigma = 1, \alpha = 0.25$)

the 10^{th} order Padé approximation. In case of the B-spline wavelet, $\widehat{t}$-transformation performs the best for orders 7 and 8, while $\widehat{\tau}$-transformation performs the best for orders 9 through 11 as seen from figure 3.5(c). The 10^{th} order $\widehat{\tau}$-transformation can be

clearly seen to be performing on par with the 11^{th} order Padé approximation. For the exponential spline wavelet, $\widehat{t}$-transformation performs the best for orders 7 through 9, while $\widehat{\tau}$-transformation performs the best for orders 10 and 11 as seen from figure 3.5(d). The 9^{th} order $\widehat{u}$, $\widehat{t}$ and $\widehat{\tau}$-transformations can be clearly seen to be performing on par with the 11^{th} order Padé approximation, which is a notable advantage of the proposed variants.

While Padé approximation has been shown to be a very special case of nonlinear sequence transformation under some conditions [83], it should be remembered that there are substantial differences between the sequence transformations and Padé approximation. For example, Levin and Weniger transformations are obtained with the help of explicit expressions whereas Padé approximation is obtained by solving a system of equations.

3.4.2 Comparison with the L_2 Method

It has been shown in [84] that for a given order, L_2 method gives better MSE when compared to the Padé method. The same is true for the proposed variants also. That is, L_2 method still performs better than the proposed variants as seen from figure 3.6 which plots the MSE of L_2 method and the best among the four proposed variants for a given order for different wavelets. However, an extra step of model reduction [85] applied on any of the medium order $(14-20)$ proposed variants to the required lower

order improves the accuracy. figure 3.6 also provides a comparison between the MSEs of the rational approximations obtained by balance and truncate model reduction of one of the medium order variants and the L_2 method. It may be mentioned here that the L_2 approximation is obtained using the RARL2 toolbox [86].

The proposed variant used, the medium order from which it is reduced and the corresponding p and β values for different wavelets are given in Table 3.7. In case of the Gaussian wavelet, for orders such as 4 and 5 the MSE values of the reduced variant and the L_2 method are so close that any difference is of no consequence from an implementation point of view, as seen from figure 3.6(a). However, in some cases the difference in MSE is notable. The 6^{th} order model reduced approximation has a value of MSE better than that of 7^{th} order obtained by the L_2 method. Similarly, for the Mexican Hat wavelet in figure 3.6(b), the L_2 method and the model reduced $\widehat{y}$-transformation have almost the same MSE values for orders 6 and 7. However, the 9^{th} order model reduced approximation has a value of MSE better than that of 10^{th} order obtained by the L_2 method.

Table 3.7: Proposed variant, its order and corresponding p and β values used for model reduction for different wavelets

Wavelet	Variant Reduced	Order	p (β)
Gaussian Wavelet	$\widehat{\tau}$-transformation	14	6 (-6.02)
Mexican Hat Wavelet	$\widehat{y}$-transformation	16	8 (-7.79)
B-spline Wavelet	$\widehat{\tau}$-transformation	16	14 (-13.48)
Exponential-spline Wavelet	$\widehat{\tau}$-transformation	16	5 (-5.76)

For B-spline wavelet in figure 3.6(c), the model reduced approximation has a value

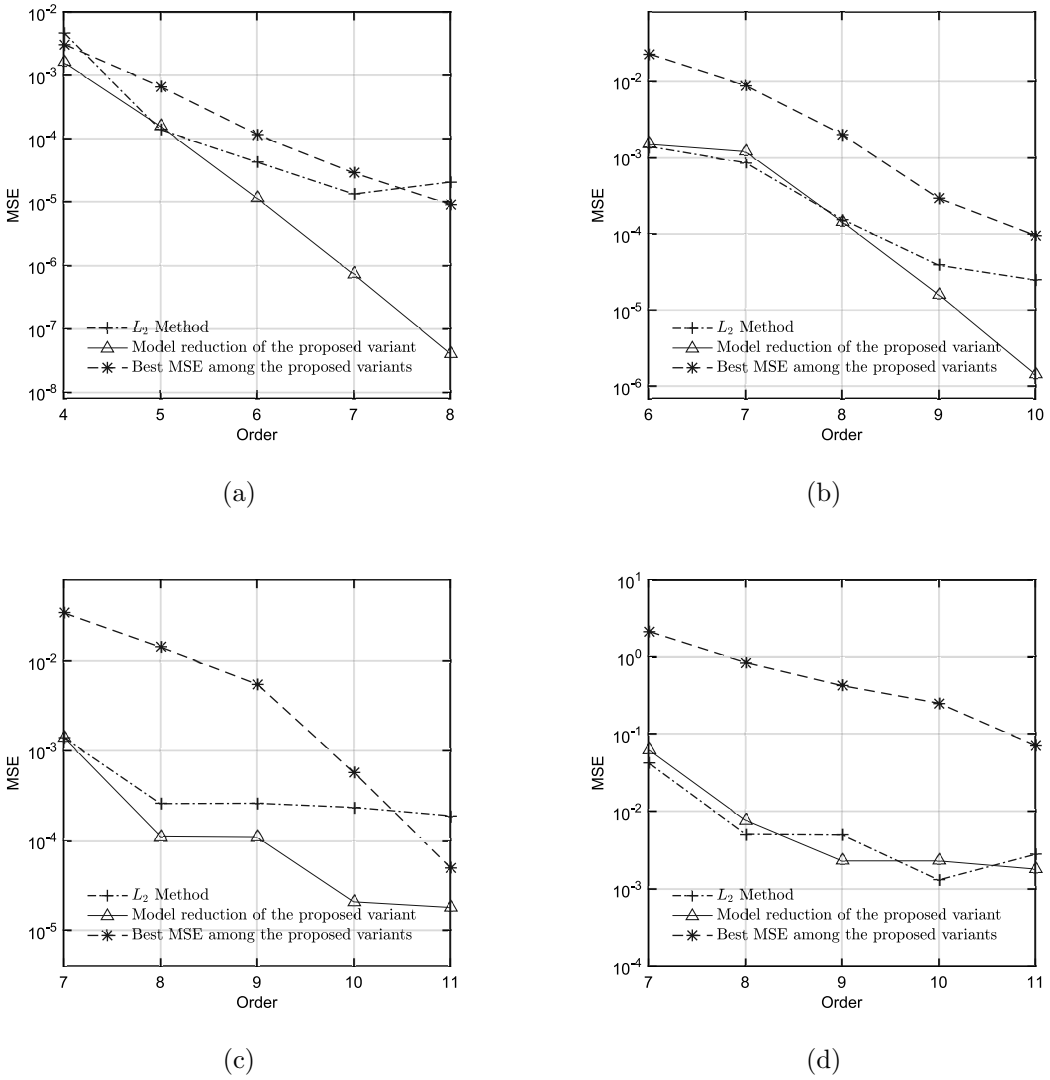

Figure 3.6: MSE versus order of approximation for L_2 method, model reduced proposed variant and best among the proposed variants (a) Gaussian Wavelet $(t_0 = 2, \sigma = 1)$ (b) Mexican Hat Wavelet $(t_0 = 3, \sigma = 1)$ (c) Third derivative of seventh order B-spline $(t_0 = 0, \sigma = 0.5)$ (d) Fourth derivative of eighth order Exponential spline $(t_0 = 0, \sigma = 1, \alpha = 0.25)$

of MSE better than that obtained by the L_2 method for orders 8 through 11. In case of the Exponential-spline wavelet, the L_2 method and the model reduced $\widehat{y}$-transformation have almost the same MSE values for all the orders 7 through 11 as seen from figure

3.6(d).

It can be argued that the approximations obtained by the Padé method can also be improved by the method discussed in this section. However, a medium order approximation obtained by the Padé method does not guarantee stability. In case of both the Gaussian and Mexican Hat wavelets, approximations obtained by the Padé method for orders above 10 have been found to be unstable. In case of B-spline and Exponential-spline wavelets, approximations obtained by the Padé method for orders above 11 have been found to be unstable.

3.4.3 Proposed Variants as Alternate Starting Points

Approximations obtained by optimization methods that rely on local search routines, like the L_2 method, depend largely on the starting points. Different starting points result in different solutions after optimization and a good starting point may help in avoiding local optima. Having several starting points gives flexibility to designers in picking a solution. The rational approximations generated by the proposed variants can also act as alternate starting points for optimization routines.

The same medium order calculated for each wavelet in the Table 3.7 is given as alternate starting point along with a same order starting point by the method described in [1] and the resulting MSEs are shown in figure 3.7. From figure 3.7(a), 3.7(b) and

3.7(d), it is clear that the proposed variant and the method in described in [1] give similar MSEs for Gaussian, Mexican Hat and Exponential-spline wavelets. However, for the B-spline wavelet, it can be seen that the proposed variant as starting point gives much better MSEs for orders 8 through 11 as seen from figure 3.7(c).

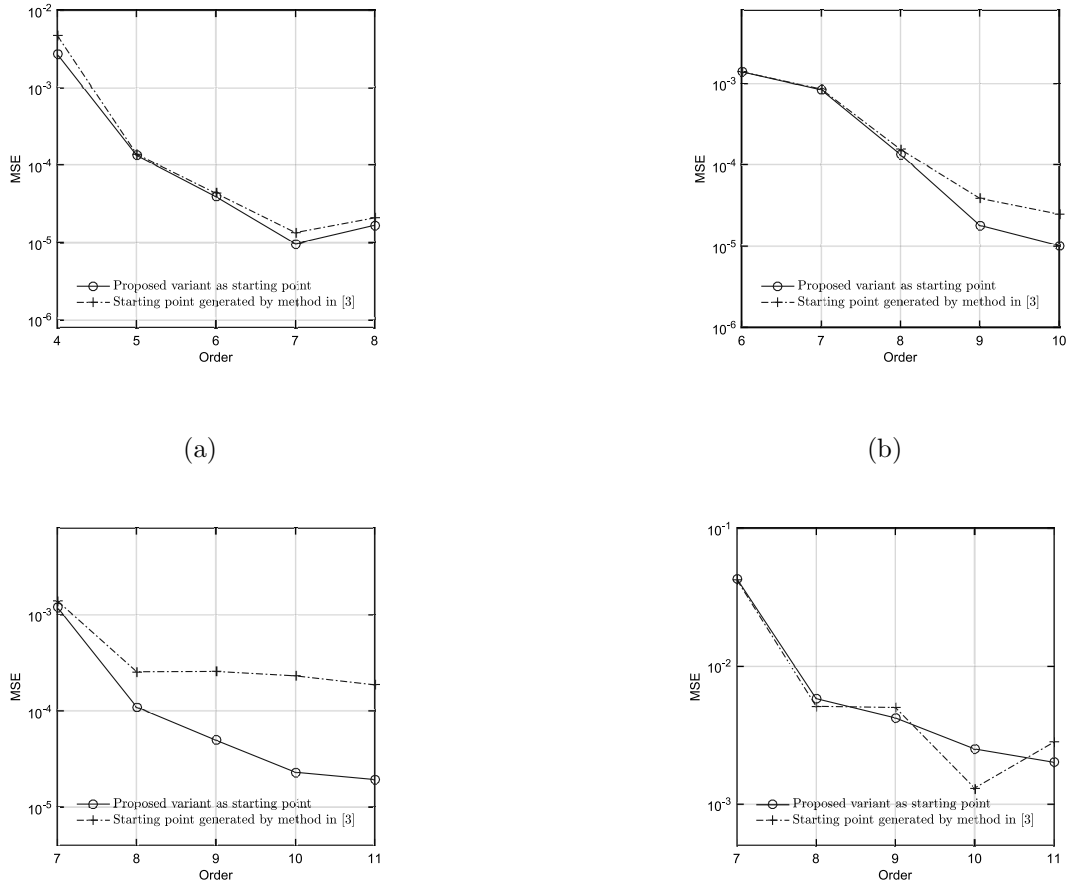

Figure 3.7: MSE versus order of approximation for L_2 method with proposed variant and method described in [1] as starting points (a) Gaussian Wavelet ($t_0 = 2, \sigma = 1$) (b) Mexican Hat Wavelet ($t_0 = 3, \sigma = 1$) (c) Third derivative of seventh order B-spline ($t_0 = 0, \sigma = 0.5$) (d) Fourth derivative of eighth order Exponential spline ($t_0 = 0, \sigma = 1, \alpha = 0.25$)

3.5 Conclusion

New variants of nonlinear sequence transformation to approximate wavelet filters have been proposed in this chapter. These variants identify irregular leading Taylor coefficients and discount them in constructing denominator polynomials of the wavelet filter transfer function. The proposed variants have explicit expressions which result in closed-form solutions. When compared to the Padé method, at least two variants have outperformed it for a given order depending on the wavelet considered. It has also been shown that the model reduced approximation of the proposed variants performs as well as the L_2 method for lower orders $(4-7)$ and better for higher orders $(8-11)$. It has been shown that these variants can also be useful as alternate starting points to the L_2 optimization routine.

Chapter 4

Closed-Form Design of Continuous-Time Linear-Phase Selective Filters

Design of continuous-time linear-phase selective filters demands rectangular magnitude and linear-phase response requiring a multi-objective optimization approach involving trade-offs. Earlier work focused on optimizing a combination of frequency domain characteristics like equiripple pass-band with linear-phase [87–89], equiripple pass-band with flat group delay [90, 91], monotonic pass-band with sharp cut-off characteristic [92, 93], monotonic pass-band with flat group-delay [94], sharp cut-off characteristic with equalized group-delay [95], equiripple pass-band and stop-band characteristics

with group-delay equalization [96], monotonic or ripples of arbitrary width in pass-band with group-delay maximally flat or equiripple in whole or part of pass-band [97] etc. Later, it has been found that the time-domain properties of these filters, such as, impulse response symmetry [38, 98] and distortion [39] help in formulating much simpler optimization criteria. Such an approach leads to a successful time-domain synthesis of linear-phase selective filters [24–26]. Time-domain synthesis has also been successfully used for approximating wavelet filters [1, 22, 23] and pulse forming and shaping networks [27–29]. While modern optimization techniques offer optimal solutions to design both discrete and continuous-time filters, closed-form solutions are also pursued [99] because they are easy to design and can act as starting points to optimization methods that rely on initial approximations.

Time-domain based closed-form solutions for linear-phase selective filters are present in discrete-domain [99] but the same for continuous-time domain are not present to the knowledge of the authors. Closed-form continuous-time filters in general can be obtained by approximating the transfer function of a linear time invariant system to a proper rational function with required impulse response using techniques like Padé approximation [45] and nonlinear sequence transformation discussed in the previous chapter. However extending this technique for the synthesis of linear-phase selective filters will result in rational functions that have complex co-efficients, making their implementation difficult [73]. This is because the Taylor co-efficients of transfer functions of such filters are complex.

In this chapter, a time-domain based closed-form design of continuous-time linear-phase selective filters is attempted for the first time. It involves expressing Laplace transform of the impulse response of linear-phase selective filters as a sum of shifted and scaled causal splines. Causal splines are considered in this work because their Laplace transforms can be calculated easily and also they have Taylor expansions with real co-efficients. The resulting expression is approximated to a rational form of medium order $(15-20)$ using variants of nonlinear sequence transformation proposed in the previous chapter which is then reduced to a desired order using balance and truncate method [85].

4.1 Causal B-splines

Causal B-splines [100] are a result of n-fold convolution of the rectangle function given by

$$\beta_{+}^{0}(t) = \begin{cases} 1 & 0 \leq t \leq 1 \\ 0 & otherwise \end{cases} \tag{4.1}$$

The Laplace transform of a n^{th} order causal B-spline is easily calculated by the convolution property and is given as

$$LT[\beta_+^n(t)] = B_+^n(s) = \left[\frac{1-e^{-s}}{s}\right]^{n+1} \tag{4.2}$$

The time-domain equation of a n^{th} order causal B-spline is calculated by taking the inverse Laplace transform of (4.2) instead of calculating the n-fold convolution and it is given as

$$\beta_+^n(t) = \frac{1}{n!}\sum_{k=0}^{n+1}(-1)^k \begin{pmatrix} n+1 \\ k \end{pmatrix} (t-k)_+^n \tag{4.3}$$

The above equations represent the classic B-splines when the order of convolution n is a positive integer ($n \geq 0$). This however differs slightly when we try to define a fractional spline [101]. Because only causal splines are considered, we can obtain the corresponding Laplace transform and time-domain equations of fractional splines with only slight modifications to the equations (4.2) and (4.3). These are given by equations (4.4) and (4.5) respectively, where α is the fractional order:

$$B_+^\alpha(s) = \left[\frac{1-e^{-s}}{s}\right]^{\alpha+1} \tag{4.4}$$

$$\beta_{+}^{\alpha}(t) = \frac{1}{\Gamma(\alpha+1)} \sum_{k=0}^{+\infty} (-1)^k \binom{\alpha+1}{k} (t-k)_{+}^{\alpha} \tag{4.5}$$

There are however two important differences between a fractional spline and a classic spline. First is the axis of symmetry. While equation (4.2) represents a symmetric spline for every positive integer, same is not true with equation (4.4). Second difference is the compact support. While classic splines are compactly supported, fractional splines are not so but decay in proportion to $|s|^{-\alpha-2}$ [101].

4.2 Proposed Method

The impulse response $h(t)$ of a linear-phase selective filter is a symmetric sinc pulse [26] given by

$$h(t) = \begin{cases} 0 & t < 0 \\ \omega_c \text{sinc}[\omega_c(\text{t} - \text{T}_0)] & 0 < t \leq 2T_0 \\ 0 & t > 2T_0 \end{cases} \tag{4.6}$$

where ω_c is the cut-off frequency, T_0 is the delay and $\text{sinc}(x) = \sin(x)/x$ for $x \neq 0$ and 1 for $x = 0$. Let us assume that the impulse response required is as shown in figure 4.1, with cut-off frequency (ω_c) chosen as 1 rad/sec (4.6). The idea is to develop an expression for the main lobe and each of the side lobes of the response individually

in the interval $0 < t \leq 2T_0$ using causal splines, both classic and fractional, and add them up to form a final expression.

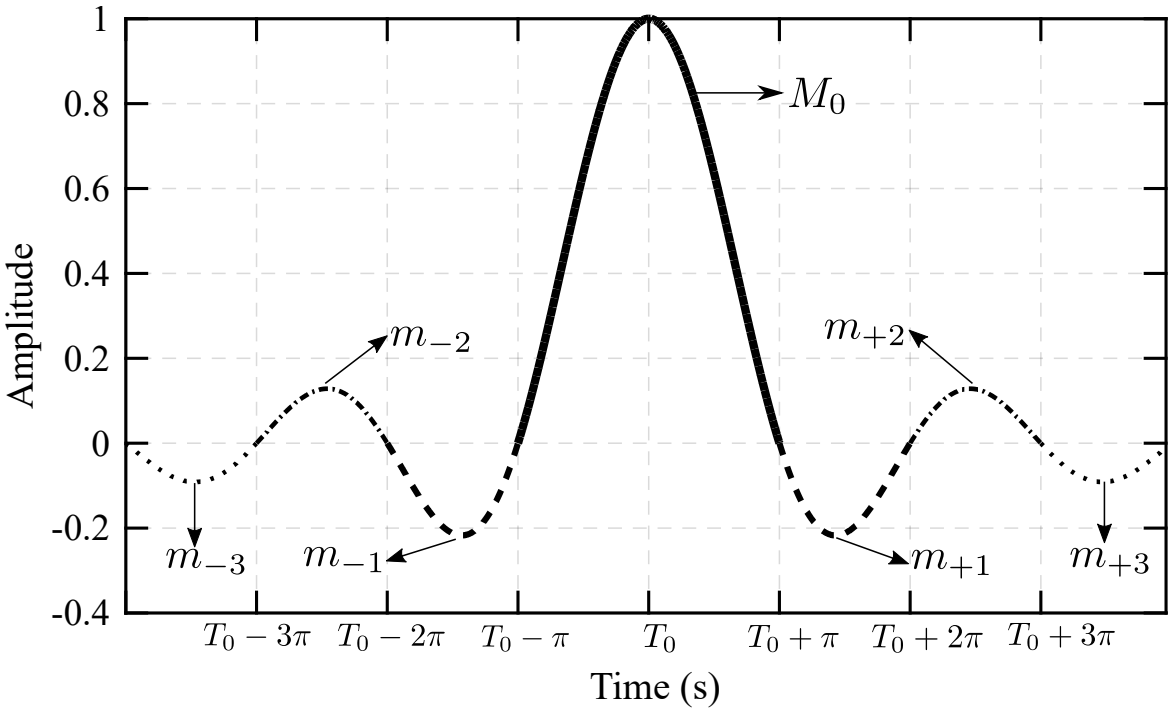

Figure 4.1: Required Symmetric Sinc pulse with delay T_0 and cut-off frequency $\omega_c = 1$ rad/sec.

It can be seen from figure 4.1 that the main lobe M_0 of the required impulse response is symmetric around T_0 with a width 2π and amplitude 1. Since the main lobe is symmetric, it can be approximated by a classic-spline. Thus, Laplace transform of M_0 can be written as a scaled and shifted classic causal B-spline of the order 1 given

by

$$M_0(s) = \pi \left[\frac{1 - e^{-\pi s}}{\pi s}\right]^2 e^{-(T_0 - \pi)s} \tag{4.7}$$

Note that the B-spline in equation (4.7) is scaled and multiplied by π so that the main lobe's width and amplitude are 2π and 1 respectively. It is also multiplied by $e^{-(T_0-\pi)s}$ to achieve the shift of $T_0 - \pi$ so that it is centered around T_0.

Now the side lobe immediately to the right of the main lobe, m_{+1} and immediately to the left of the main lobe, m_{-1}, are to be defined. It is clear from figure 4.1 that both the side lobes m_{+1} and m_{-1} have a width of π, amplitude of -0.217 but do not have an axis of symmetry. Thus, these two side lobes can be expressed with the help of a fractional spline of the order $\alpha + 1 = \pi$, whose maximum amplitude is ≈ 0.75. Since the absolute maximum value of the side lobes m_{+1} and m_{-1} occurs approximately at $T_0 + \frac{3\pi}{2}$ and $T_0 - \frac{3\pi}{2}$ respectively, we can define the Laplace transform of side lobes m_{+1} and m_{-1} as

$$m_{+1}(s) \approx \frac{\mathrm{sinc}[\frac{3\pi}{2}]}{0.75} \left[\frac{1 - e^{-s}}{s}\right]^{\pi} e^{-(T_0 + \pi)s} \tag{4.8}$$

$$m_{-1}(s) \approx \frac{\mathrm{sinc}[\frac{3\pi}{2}]}{0.75} \left[\frac{1 - e^{-s}}{s}\right]^{\pi} e^{-(T_0 - 2\pi)s} \tag{4.9}$$

These side lobes are shifted by appropriate amounts so that they occur just before and

after the main lobe. Similarly, the side lobes m_{+2} and m_{-2} are expressed as shifted and scaled versions of causal fractional splines similar to equations (4.8) and (4.9). Finally, the Laplace transform of each lobe in the interval $0 < t \leq 2T_0$ is calculated and summed up to obtain the expression for Laplace transform of the required impulse response (4.10).

$$H(s) = \ldots + m_{-2}(s) + m_{-1}(s) + M_0(s) + m_{+1}(s) + m_{+2}(s) + \ldots \tag{4.10}$$

The delay T_0 in equation (4.6) is chosen to be at least 2π so that symmetry exists. Thus, the generalized expression for transfer function of linear-phase selective filter $H(s)$ with delay $T_0 = p\pi, p \geq 2$ is given as in equation (4.11) below.

$$\begin{aligned} H(s) = & \underbrace{\pi \left[\frac{1-e^{-\pi s}}{\pi s}\right]^2 e^{-(p-1)\pi s}}_{\textbf{Main lobe}} \\ & + \underbrace{\sum_{k=1}^{p-1} \frac{\operatorname{sinc}[(2k+1)\frac{\pi}{2}]}{0.75} \left[\frac{1-e^{-s}}{s}\right]^{\pi} e^{-(p+k)\pi s}}_{\textbf{Side lobes to the right of main lobe}} \\ & + \underbrace{\sum_{k=1}^{p-1} \frac{\operatorname{sinc}[(2k+1)\frac{\pi}{2}]}{0.75} \left[\frac{1-e^{-s}}{s}\right]^{\pi} e^{-(p-(k+1))\pi s}}_{\textbf{Side lobes to the left of main lobe}} \end{aligned} \tag{4.11}$$

4.2.1 Magnitude and Phase properties of the Proposed Filter

Equation (4.11) given earlier provides an approximation to the Laplace transform of the impulse response of linear-phase selective filters. The expressions governing the

magnitude $|H(j\omega)|$ and phase $\angle H(j\omega)$ of the proposed transfer function are given in (4.12) and (4.13).

$$|H(j\omega)| = \frac{2}{0.75}\left|\text{sinc}(\frac{\omega}{2})\right|^{\pi}\sum_{k=1}^{p-1}\left|\text{sinc}((2k+1)\frac{\pi}{2})\right| + \pi\left|\text{sinc}(\frac{\pi\omega}{2})\right|^{2} \tag{4.12}$$

$$\underline{/H(j\omega)} = -p\pi\omega + \frac{\pi^2\omega^2}{2}(2p-1) \tag{4.13}$$

From the above equations it is clear that the magnitude approximates a rectangular function as depicted in figure 4.2(a) for p=4. Also the phase is a linear function of frequency in the pass-band as shown in figure 4.2(b). From the figure 4.2 it is clear that equation (4.11) produces the required magnitude and phase responses for linear-phase selective filters. However, this transfer function is not in a practically realizable form and needs to be converted to a proper rational function. Since the motivation of this work is to obtain a closed-form solution, we opt for $\widehat{y}$-transformation proposed in the previous chapter to obtain a medium order $(15-20)$ approximation, which is subsequently balanced and truncated to obtain the linear-phase selective filter of required order. Getting a (given) k^{th} order approximation from equation (4.11) depends on two factors: i) The delay T_0 which is characterised by p in (4.11) and ii) The medium order $k_{n,m}$, where n and m are degrees of numerator and denominator respectively, from which the required k^{th} order is to be obtained. Table 4.1 describes

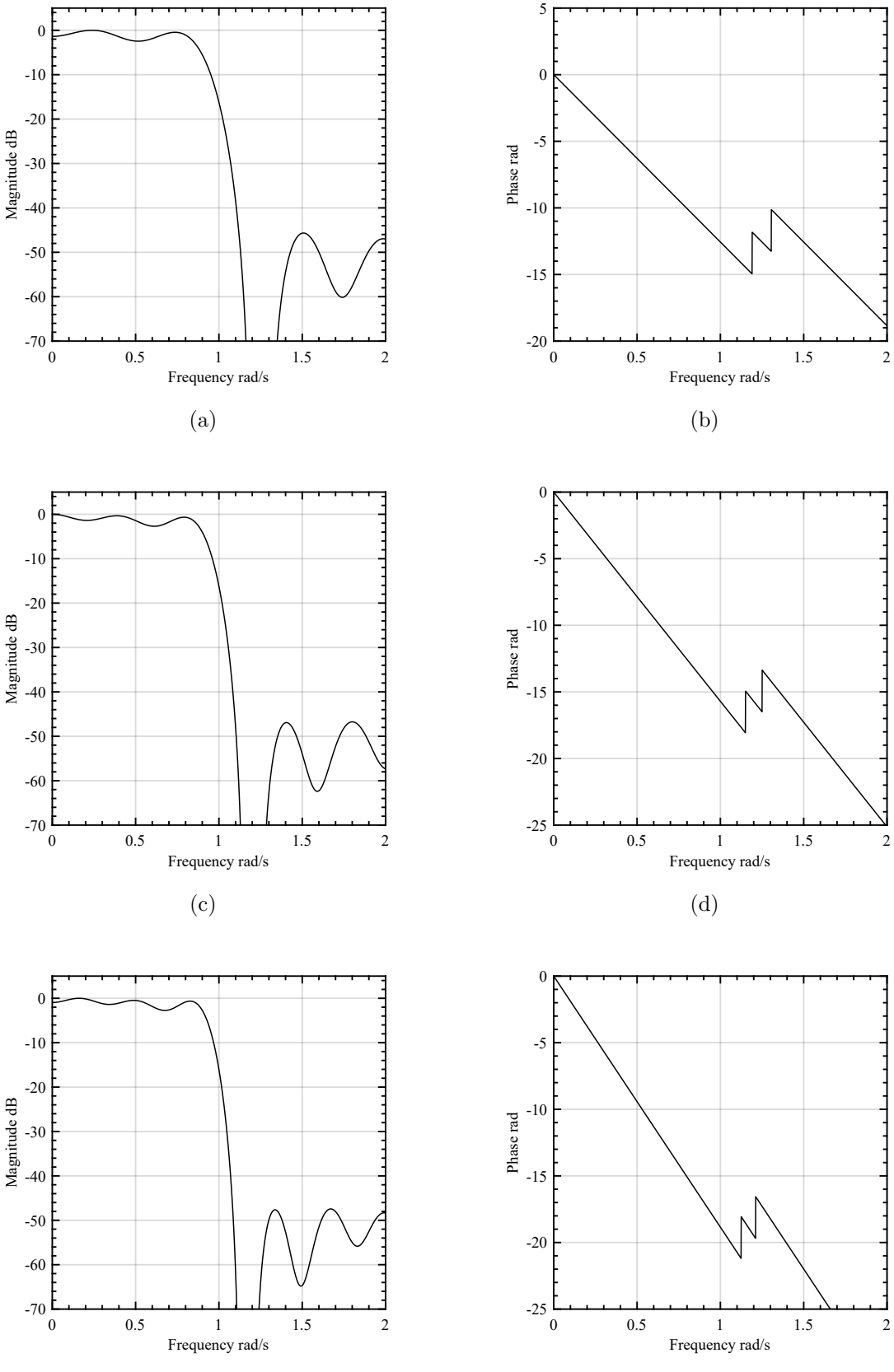

Figure 4.2: Magnitude and Phase response of the proposed transfer function for p=4 (a) Magnitude response (b) Phase response

two parameters p and $k_{n,m}$ used to obtain the k$^{\text{th}}$ order approximation. These two parameters are chosen such that the Hankel singular value of the reduced order is less than 0.1 except for lower orders 3 to 5 for which it is taken as 0.5.

Table 4.1: The values of p and the medium order $k_{n,m}$

Order of Approximation (k)	Delay Parameter (p)	Medium Order ($k_{n,m}$)
3	2	[11,13]
4	2.5	[11,13]
5	3	[12,14]
6	3.5	[12,14]
7	4	[13,15]
8	4.5	[13,15]
9	5	[14,16]
10	5.5	[14,16]
11	6	[15,17]
12	6.5	[15,17]

4.3 Properties of the Proposed Filters

Continuous-time linear-phase selective filters with ω_c of 1 rad/sec are synthesized using the proposed method and their properties studied in this section. Figure 4.3 shows the magnitude and phase responses of the proposed filters. Figure 4.3(a) gives the responses for orders $4, 5$ and 7 while figure 4.3(b) and figure 4.3(c) provide the same for orders 7 to 9 and 10 to 12 respectively. It can be seen clearly from the figures that the magnitude response approximates a rectangle function, with ripples of arbitrary width in the pass-band. Further, it is clear from figure 4.3(b) that for $k \geq 6$ the pass-band ripple is less than 2 dB. Similarly, it can be seen from figure 4.3(c) that for $k \geq 9$, the pass-band ripple is around 0.5 dB. For a given k$^{\text{th}}$ order, the proposed filters result in k poles and $k-1$ zeros. Because of the zeros we can observe notches in the

stop-band responses in figure 4.3(a) to 4.3(c). Figure 4.3(d) gives the phase responses of the proposed filters form $k = 4$ to $k = 12$. It is clear from this figure that the phase response is linear in the passband as required. The slope of the phase responses can be seen to be increasing as the order of the filter is increased. This is because the delay parameter p is increased as the filter order is increased. Figure 4.4 shows the impulse responses of the proposed filters of the orders 4 to 12. As desired, the impulse responses almost mimic the required symmetric sinc responses.

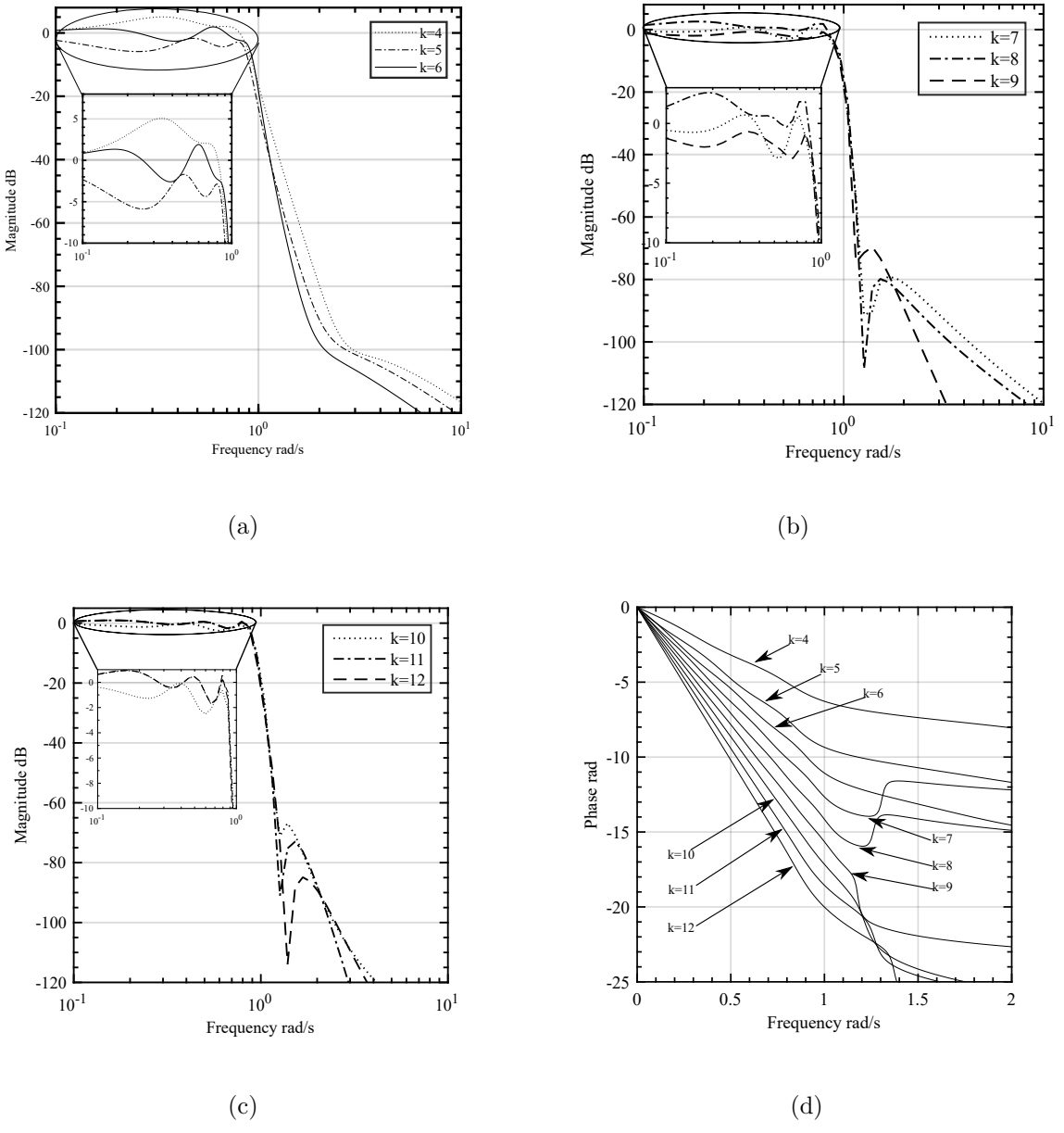

Figure 4.3: Magnitude and responses of proposed filter normalized to $\omega_c = 1$ rad/sec (a) Magnitude responses for orders $4, 5$ and 6 (b) Magnitude responses for orders $7, 8$ and 9 (c) Magnitude responses for orders $10, 11$ and 12 (d) Phase responses for orders 4 to 12

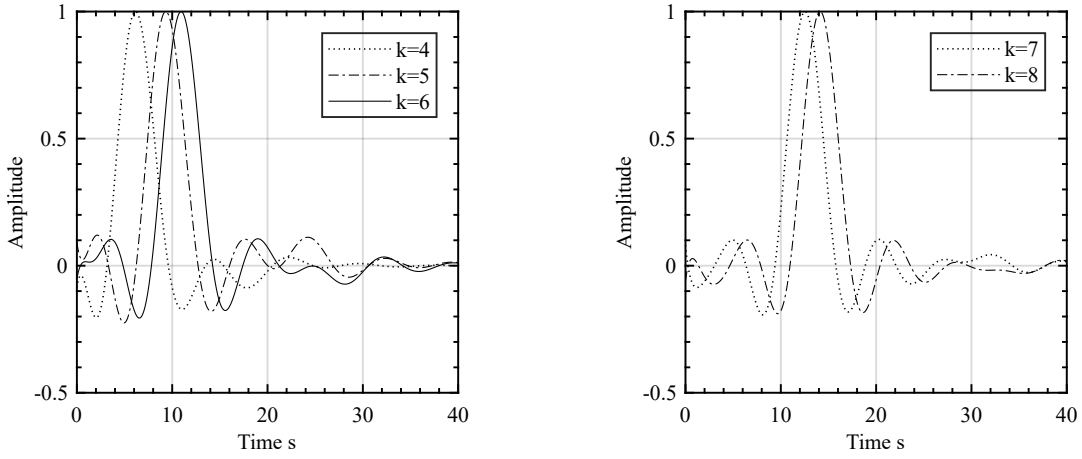

(a)

(b)

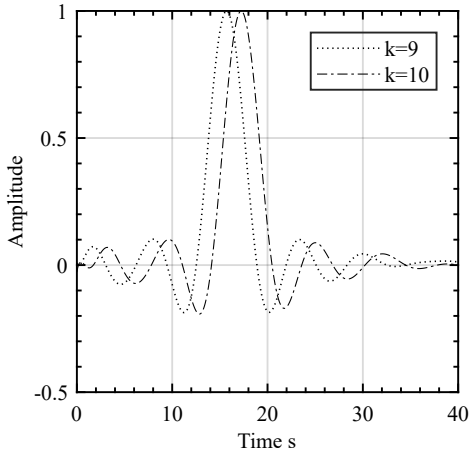

(c)

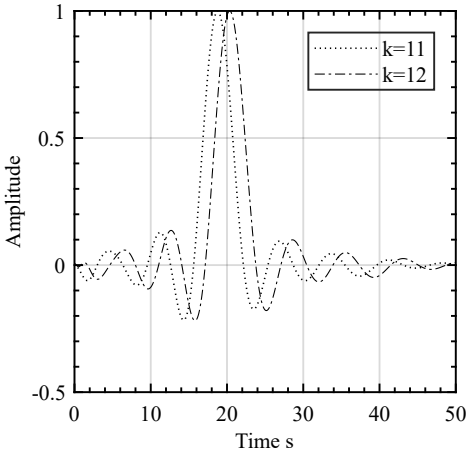

(d)

Figure 4.4: Impulse responses of the proposed filter (a) Orders $4, 5$ and 6 (b) Orders 7 and 8 (c) Orders 9 and 10 (d) Orders 11 and 12

4.4 Comparison With L_2-Method

Since there are no other time-domain based closed-form solutions for linear-phase selective filters, the proposed method is compared to the L_2 method, an iterative procedure that optimizes the L_2 norm between the approximation and the required impulse response. The L_2 optimization is carried out by the toolbox given in [86]. Figure 4.5 shows the comparison of the magnitude and phase characteristics of the proposed method and the L_2 method for orders 5, 7 and 9. From figure 4.5(a), it is clear that the 5^{th} order filter obtained by the proposed method has larger ripple in the pass-band when compared to the L_2 method. However, the proposed method has a steeper cut-off characteristic, resulting in a better stop-band characteristic. The ripple in the pass-band for both the methods is similar for 7^{th} and 9^{th} order filters as seen from the figure 4.5(b) and 4.5(c) respectively. While the stop-band notch is much deeper for the 7^{th} order filter obtained by the L_2 method when compared to the proposed filter, it is same for both the methods for 9^{th} order filters. The phase characteristics obtained by both the methods are similar and linear in the pass-band as seen from figure 4.5(d).

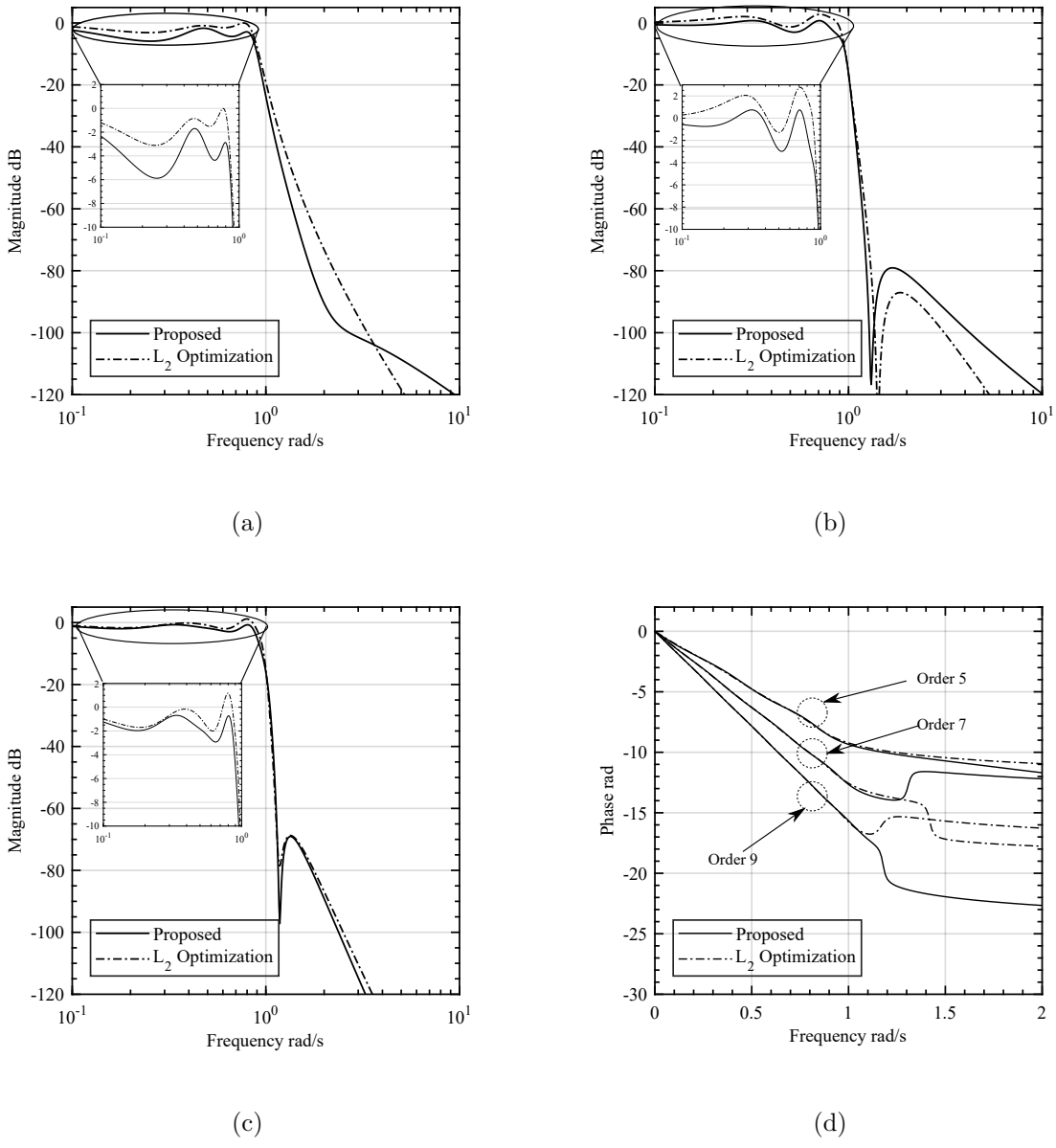

Figure 4.5: Comparison of the proposed method with L_2 method (a) 5^{th} order magnitude responses (b) 7^{th} order magnitude responses (c) 9^{th} order magnitude responses (d) Phase response comparison for orders 5, 7 and 9

4.5 Proposed Method as a Starting Point

Solutions obtained by optimization methods that rely on local search routines depend largely on the starting points. Different starting points result in different solutions after optimization and a good starting point may help in avoiding local optima. Having several starting points gives flexibility to designers in picking a solution. In [1], an automated procedure for generating starting points before doing L_2 optimization has been presented. This procedure involved model reduction of a higher order discrete-time FIR filter to a medium order IIR filter which was then converted to continuous-time and finally reduced to the required lower order.

The solution generated by the proposed method can also act as an alternate starting point for optimization routines. Figure 4.6 shows a comparison of 9^{th} order filter responses obtained after L_2 optimization, whose starting points are given by the method in [1], and those by the proposed method. While the proposed method results in a ripple of around 0.85 dB in the passband, the method proposed in [1] has a ripple of around 1.4 dB. However, the starting point obtained through the proposed method results in a deeper notch in the stopband compared to that given by the method in [1]. As seen from figure 4.6(b), both methods result in linear-phase in the passband as required. A designer can therefore choose among the two solutions depending on the passband and stopband characteristics required.

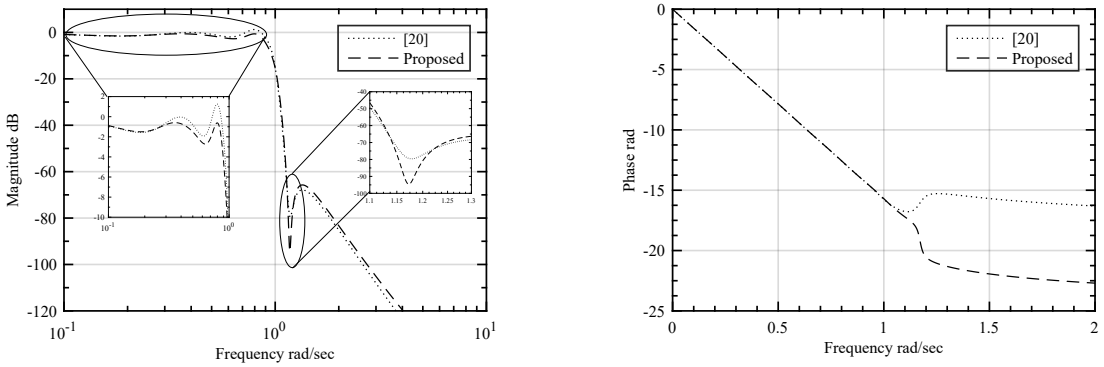

(a) (b)

Figure 4.6: Comparison of responses of the 9^{th} order filters after L_2 optimization using different starting points (a) Magnitude response (b) Phase response.

4.6 Conclusion

In this chapter we proposed a time-domain closed-form solution to design continuous-time linear-phase selective filters using the sum of shifted and scaled causal splines. This method demonstrated the required characteristics of rectangular magnitude and linear phase response. While it has been shown that the proposed method compares well with the L_2 method, it is also clear that the closed-form solution can also act as an alternate starting point for optimization methods that use local search routines.

Chapter 5

Circuit Implementation

The final step in time-domain synthesis of continuous-time filters is the practical implementation of the transfer function $H(s)$ obtained using the techniques mentioned in previous chapters. The electrical network that mimics the transfer function is not unique and there are several ways in which it can be implemented. Although this thesis concentrates mainly on the approximation problem in time-domain synthesis, we also demonstrate that the transfer functions obtained by the proposed variants can in fact be translated in to electrical networks. This is done by simulating a filter, approximating a Gabor wavelet, as a G_m-C network.

5.1 Circuit Implementation of Gabor Wavelet

In this section, a continuous-time analog circuit implementation of Gabor wavelet, whose transfer function is approximated by making use of one of the proposed variants of nonlinear sequence transformation, is presented. The Gabor wavelet is obtained by multiplying a complex exponential with a Gaussian window function as given in the equation below

$$\psi(t) = w(\tau - t)e^{-i2\pi ft} \tag{5.1}$$

$$w(\tau) = \frac{1}{\sigma\sqrt{2\pi}}e^{-\frac{\tau^2}{2\sigma^2}} \tag{5.2}$$

From the equation of the Gabor wavelet described in (5.1), the impulse response of the LTI system to be implemented can be calculated and is given as

$$h(t) = e^{-i2\pi f\tau}\ \frac{|f|}{\sqrt{2\pi}}e^{-\frac{(t-\tau)^2 f^2}{2}}e^{-i2\pi f(t-\tau)} \tag{5.3}$$

From the above impulse response the transfer function of the filter is obtained as

$$H(s) = \frac{|f|}{\sqrt{2\pi}}\int_{-\infty}^{+\infty} e^{-\frac{(t-\tau)^2 f^2}{2}}e^{-i2\pi ft}e^{-st}dt \tag{5.4}$$

A good approximation of $H(s)$ in equation (5.4) is required now to make implementation feasible. Using one of the proposed variants of nonlinear sequence transformation as

described by equations (3.12) - (3.15) a stable transfer function can be obtained. On careful observation of the transfer function in equation (5.4), we can establish that the Laplace transform needs to be calculated for the Gaussian window function multiplied by $e^{-i2\pi ft}$. Therefore, the final transfer function is written with the help of convolution property as

$$H(s) = H_{gauss}(s) * H_E(s) \tag{5.5}$$

where $H_{gauss}(s)$ is the Laplace transform of the Gaussian window function, $H_E(s)$ is the Laplace transform of $e^{-i2\pi ft}$ and $*$ stands for convolution. Applying Euler's formula on equation (5.5), we can rewrite it as

$$H(s) = H_{gauss}(s) * \Big(\mathcal{L}[\cos(2\pi ft)] - j\ \mathcal{L}[\sin(2\pi ft)]\Big) \tag{5.6}$$

By using one of the proposed variants of nonlinear sequence transformation as described by equations (3.12) - (3.15) given in Chapter 3, a rational approximation for the Gaussian window can be obtained. In this work a Gaussian window shifted by 1.5 time units and at a frequency of 2 Hz is considered.

For a fifth order rational approximation, it is observed that the $H_{gauss}(s)$ obtained by using the Weniger $\widehat{y}$-transform has the least Mean Square Error (MSE) of all the four transformations and it is given as

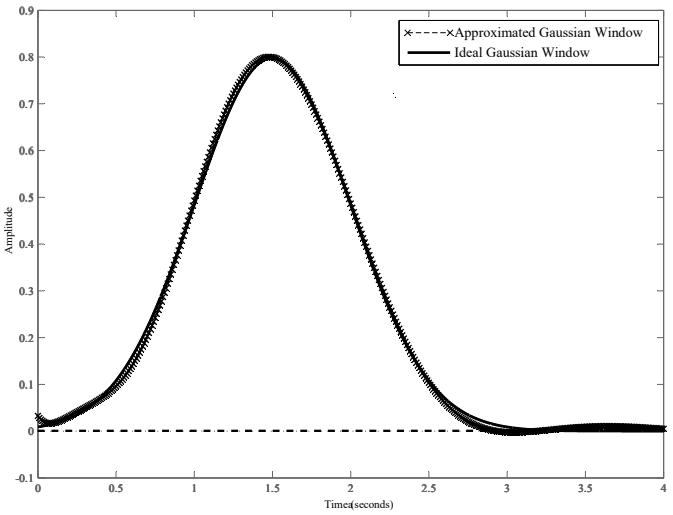

Figure 5.1: Impulse responses of the Gaussian window, the ideal impulse(solid line) and the approximated impulse(dashed line).

$$\frac{0.03242s^4 - 0.1847s^3 + 6.31s^2 - 28.86s + 167.7}{s^5 + 8.876s^4 + 44.13s^3 + 131.6s^2 + 223.3s + 167.9} \tag{5.7}$$

Figure 5.1 shows the impulse response of the approximated Gaussian window with the required ideal response. Using equations (5.6) and (5.7) we can compute the final transfer function and it should be obvious that it would have real and imaginary parts. Both the real and imaginary transfer functions have the same denominators but the numerators will vary. The final transfer function would be tenth order with 9 zeroes for real part and 8 zeroes for imaginary part as seen in equation (5.8). The impulse response of approximated imaginary and real transfer functions along with the ideal responses are shown in figures 5.2 and 5.3 respectively. From these figures it can be inferred that the approximation closely follows the required ideal waveform thus

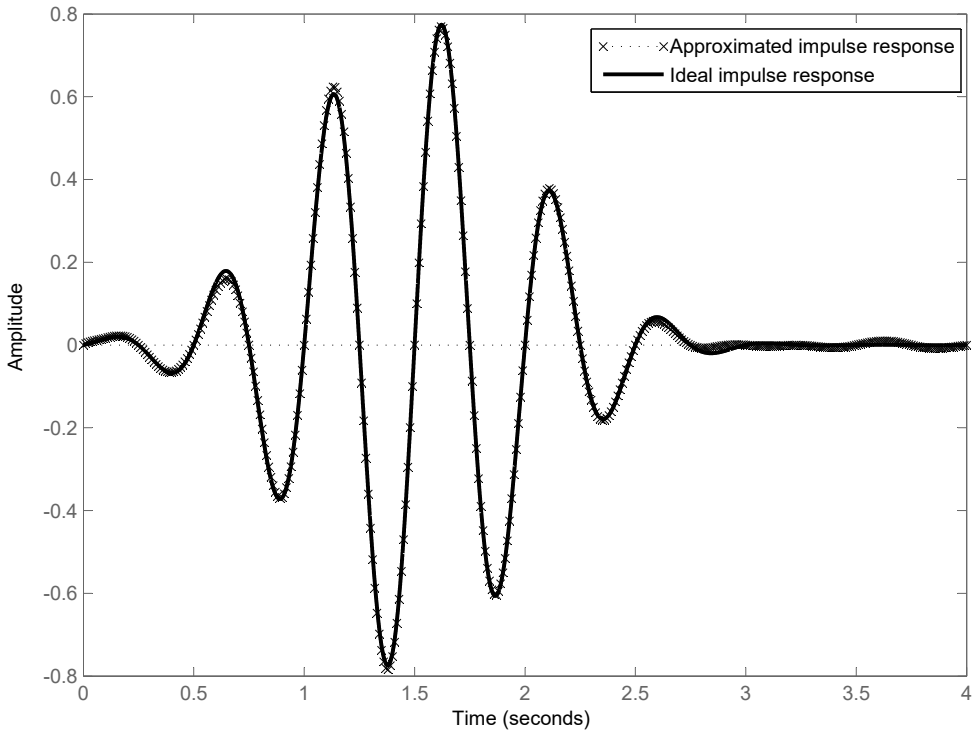

Figure 5.2: Impulse response approximation: Imaginary output

proving the Non linear sequence transformation method works very well.

$$D(s) = s^{10} + 17.75s^9 + 956.6s^8 + 1.22e04s^7 + 3.31e05s^6 + 3e06s^5 + 5.2e07s^4 + 3.07e08s^3 + 3.69e09s^2 + 1.10e10s + 9.25e10$$

$$Im(s) = 0.407s^8 - 4.64s^7 + 456.63s^6 - 2.34e3s^5 + 1.09e5s^4 + 1.07e5s^3 + 2.55e6s^2 + 3.41e7s - 5.41e6$$

$$Re(s) = 0.032s^9 + 0.10s^8 + 26.57s^6 + 146.695s^5 + 3928.32s^4 + 7.25e4s^3 - 3.92e5s^3 + 6.33e6s^2 - 1.31e7s - 3.19e6 \tag{5.8}$$

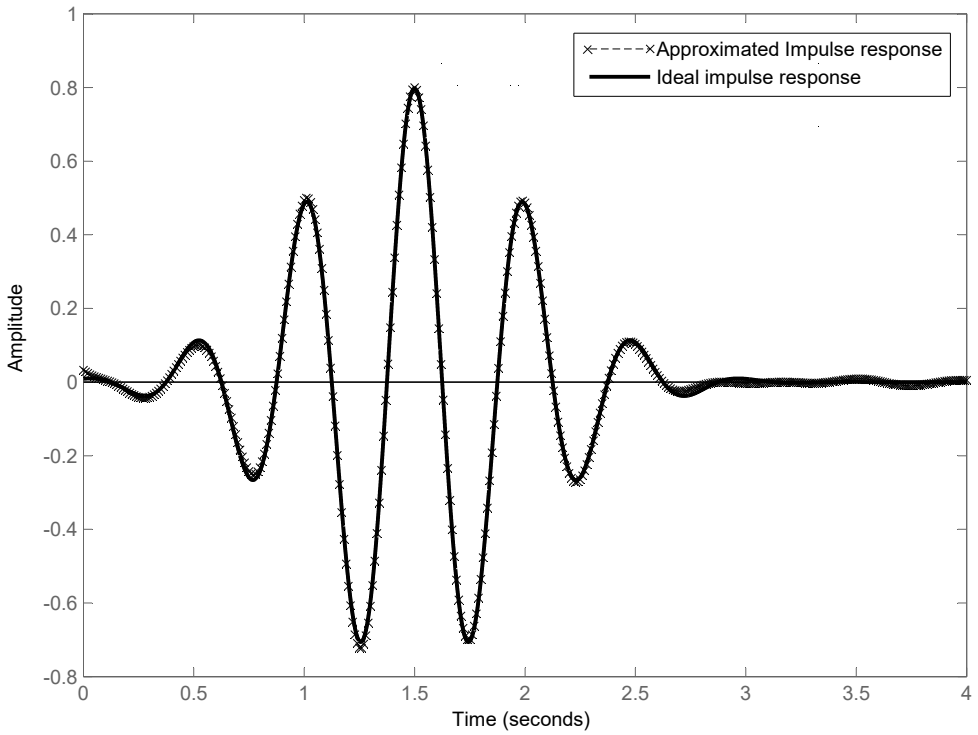

Figure 5.3: Impulse response approximation: Real output

5.2 Filter design

To prove that the approximated Gabor wavelet can be implemented, an Inverse Follow the Leader Feedback (IFLF) input distribution filter design methodology [102] is followed, for realization of both poles and zeros. This is due to its simplicity in synthesis of a generic transfer function. IFLF filters are based on OTA-C integrators as the main building blocks. All the internal circuit nodes contain a grounded capacitor in this filter structure [103].

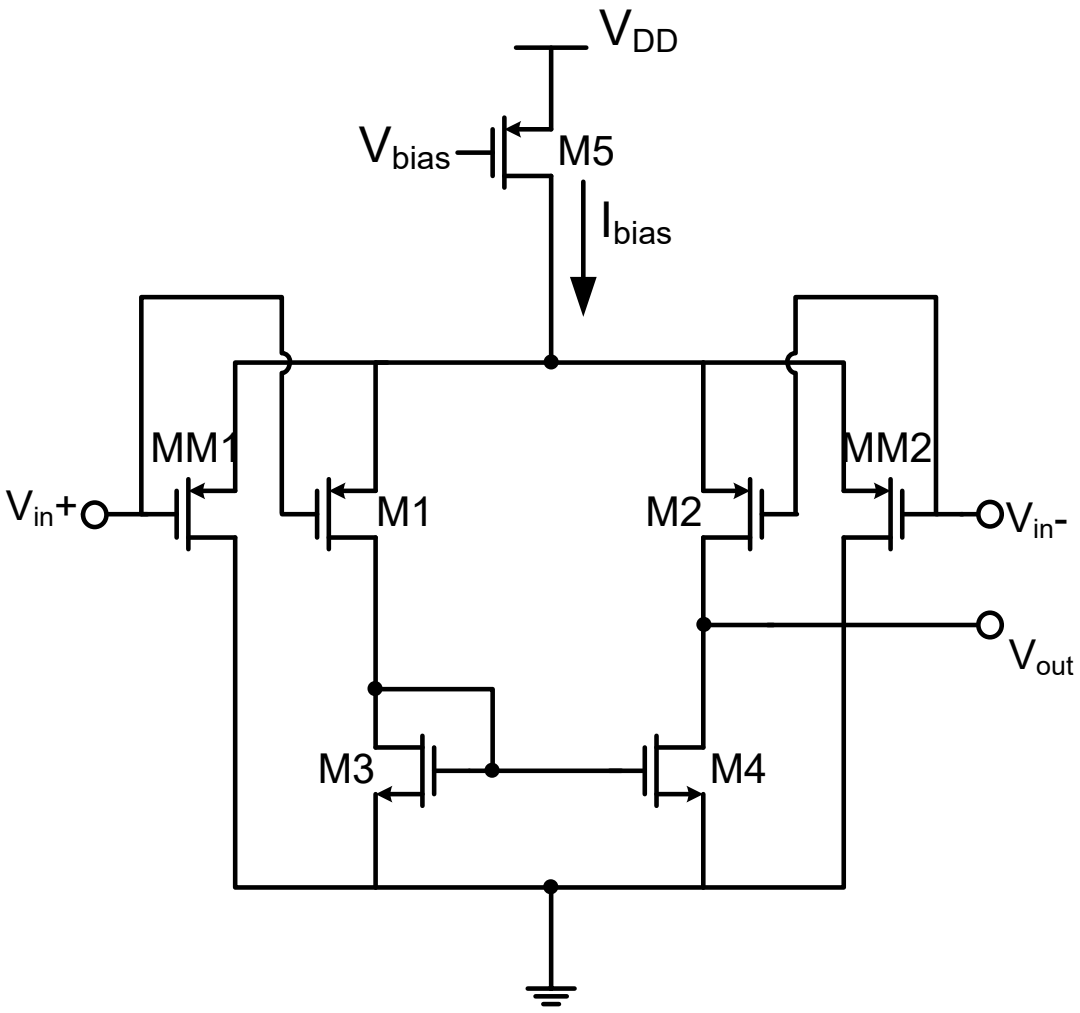

Figure 5.4: Schematic of the transconductor.

5.3 Low power transconductor circuit design

A fully integrable filter design is made possible by OTA-C filter design methodology. The transfer functions obtained in equation (5.8) have characteristics of band pass filter. The center frequency of the two transfer functions is 2 Hz as we started out with a Gaussian window which localizes a frequency of 2 Hz. This low value of center frequency results in large time constants, which require very low value of transconductances, in

the range of pS. To be able to achieve these low transconductances, very low bias currents in the range of pA are required. In [104], it is shown that bias currents in the range of fA are indeed achievable. Figure 5.4 shows the transconductor block used in the current work. It consists of a simple PMOS differential pair and employs a current division technique [105] to achieve very low transconductances as required in the present situation. All the transistors shown in figure 5.4 are operated in deep weak inversion region to obtain the lower value of the transconductances as needed.

5.4 Simulation Results

The tenth order real part of the transfer function of the Gabor wavelet filter is simulated using TSMC 0.18 μm technology with a supply voltage of 1.8 V and a total capacitance of 527.8 pF as shown in figure 5.5. The simulated magnitude response is shown along with the actual magnitude response in figure 5.6. As per the design the center frequency of the filter is observed at 2 Hz. The filter draws a total current of 4.48 nA resulting in a total power consumption of around 8 nW. The transfer function magnitude characteristics resemble that of a band pass filter with a pass band ranging from 1.74- 2.25 Hz. Since the pass band is only 0.51 Hz wide, it would be inappropriate to compute Total Harmonic Distortion (THD). Therefore, the filter distortion is quoted in terms of third order intermodulation distortion (IMD3). Sine wave inputs of 2 Hz and 2.1 Hz with an amplitude of 60.6 mV_{pp} are applied to the filter resulting in a IMD3

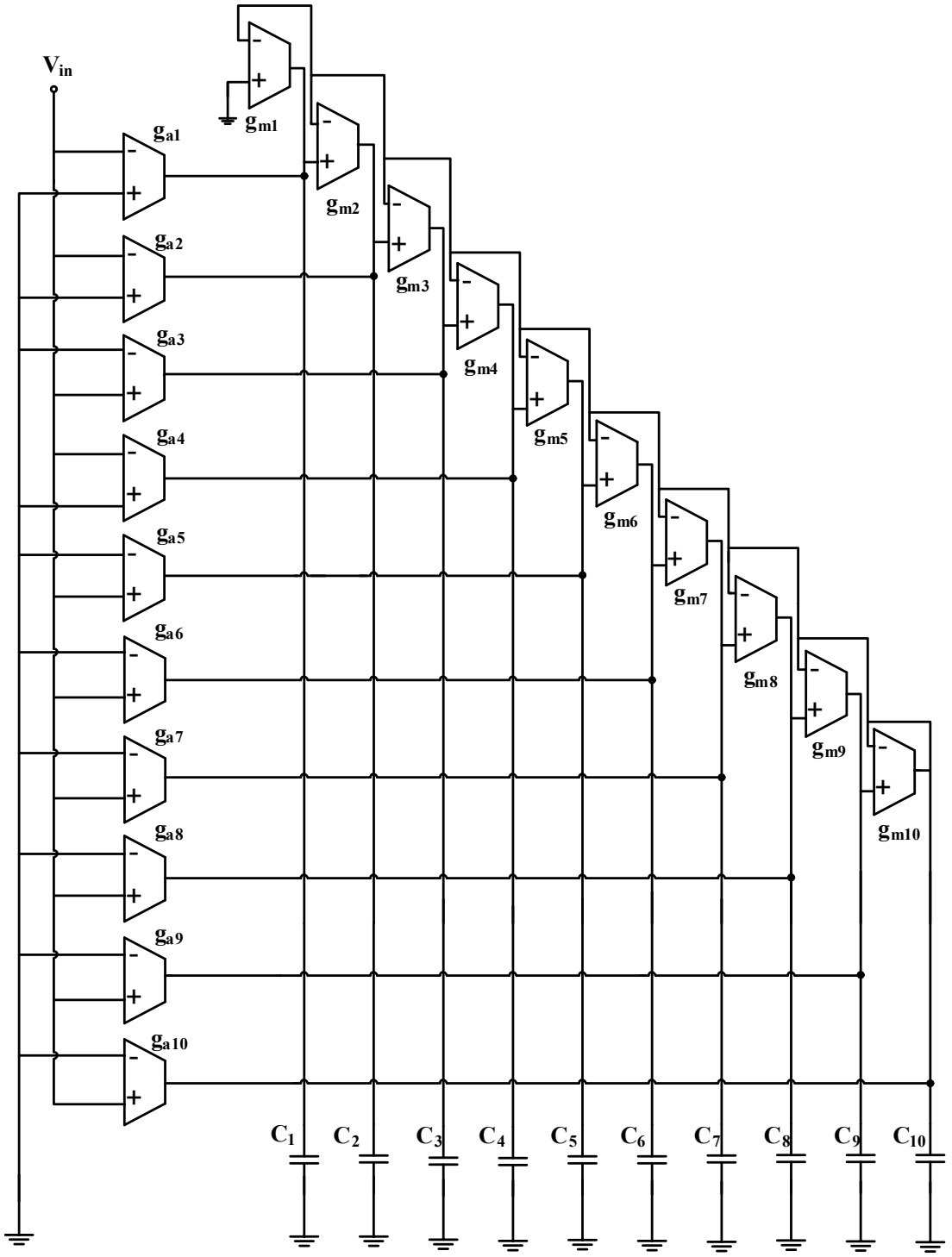

Figure 5.5: Block diagram of the Gabor wavelet-transform filter (Real Part).

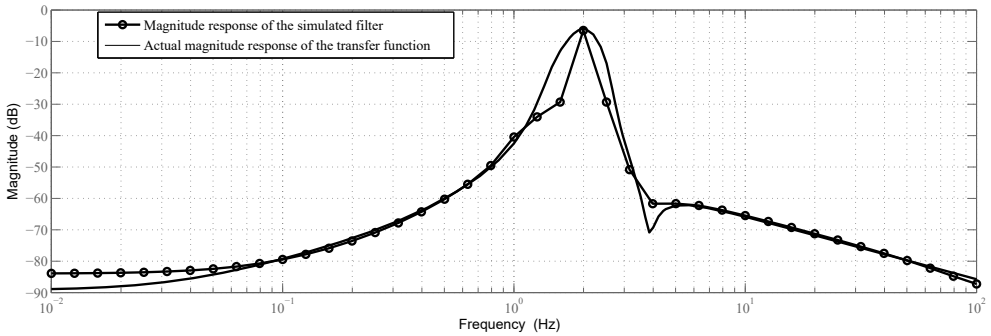

Figure 5.6: Magnitude response comparison of the designed filter with respect to magnitude response of the transfer function

of -19.99 dB with a dynamic range of 42.15 dB. Input signal levels can be up to 60.6 mV_{pp} and the input referred noise is observed to be 473.1 $\mu V/\sqrt{Hz}$. The performance of the filter is summarized in Table 5.1.

Table 5.1: Summary of simulated filter performance

V_{DD} = 1.8 V, TSMC 0.18 μm technology	
Order and Topology	10^{th} order and single ended
Supply current drawn	4.48 nA
Total capacitance	527.8 pF
Power consumption	8.07 nW
Center frequency	2 Hz
Signal input range	Up to 60.6 mV_{pp}
Input referred noise	473.1 μ V/$\sqrt{Hz}$
THD (2Hz, 60.6 mV_{pp} input)	<-29 dB
IMD3 (2, 2.1 Hz inputs 60.6 mV_{pp})	-19.99 dB
Dynamic range (for -20 dB IMD3 at output)	42.15 dB

5.5 Conclusion

In this chapter, an electrical network that implements a Gabor wavelet filter obtained by one of the proposed variants is simulated to validate the technique. IFLF input distribution filter architecture has been used for simulation. Since this architecture is based on OTA-C design methodology, a low power transconductor circuit is designed. Using this transconductor as the basic building block, a tenth order real part of transfer function of Gabor wavelet filter is simulated. Results clearly shown that the circuit closely approximates the required transfer function.

Chapter 6

Conclusions and Future Work

In this work, our prime focus has been on obtaining closed-form solutions to the time-domain synthesis approximation problem for advanced continuous-time filters such as wavelet filters and linear-phase frequency selective filters. Nonlinear sequence transformation and many of its variants have been attempted to obtain such closed-form solutions. However, due to initial irregular Taylor coefficients in the Taylor series of the transfer functions of these advanced filters, BIBO stable rational transfer functions could not be obtained. Therefore, new variants of nonlinear sequence transformation that discount the initial irregular Taylor coefficients have been proposed.

These variants have been shown to be successful in being able to approximate several mother wavelet bases like Gaussian, B-spline and E-spline wavelets. They have also been shown to be better in terms of MSE when compared to the other closed-form

method, the Pade method. It has been found that the MSEs of model order reduced transfer functions of the proposed variants are comparable to those obtained by the L_2 optimization routine. It is observed that these closed-form solutions can also act as starting points for optimization routines.

In case of linear-phase frequency selective filters, the desired impulse response is a symmetric sinc pulse. When the proposed variants were applied on the Taylor series of the Laplace transform of the sinc pulse, they resulted in rational approximations but with complex coefficients. Such complex coefficients however make practical implementation of these filters cumbersome. To achieve rational approximation with real coefficients, first the Laplace transform of the sinc pulse was approximated with the help of shifted and scaled causal splines. After obtaining this approximation, one of the proposed variants has been used to achieve a medium order approximation which is balanced and truncated to the required order to obtain the final transfer function. While it has been demonstrated that the proposed method compares well with the L_2 method, it has also been shown that the closed-form solution can act as an alternate starting point for optimization methods that use local search routines.

Finally, a Gabor wavelet filter transfer function obtained by one of the proposed variants has been simulated to validate the technique. Architecture of IFLF input distribution filter has been used for simulation. Since it is based on operational transconductance amplifier - capacitor (OTA-C) design methodology, a low power transconductor circuit has been designed. Using this transconductor as the basic

building block, a tenth order real part of transfer function of Gabor wavelet filter was simulated. Results clearly indicate that the circuit closely approximates the required transfer function.

6.1 Future Work

From an implementation perspective, it was shown in [23] that continuous-time transfer functions that have zeros only on the imaginary axis can be implemented as doubly or singly terminated ladder filters. Such filters have been shown to have good dynamic range, which is one of the crucial parameters in filter design. However, there are no generic closed-form methods that can obtain transfer functions with zeros only on imaginary axis. We plan to concentrate on approximating such transfer functions using closed-form methods, in future.

Bibliography

[1] J. M. Karel, S. A. Haddad, S. Hiseni, R. L. Westra, W. Serdijn, R. L. Peeters, *et al.*, "Implementing wavelets in continuous-time analog circuits with dynamic range optimization," *IEEE Transactions on Circuits and Systems I: Regular Papers*, vol. 59, no. 2, pp. 229–242, 2012.

[2] H. Blinchikoff and H. Krause, *Filtering in the time and frequency domains*. The Institution of Engineering and Technology, 2001.

[3] W. Kautz, "Transient synthesis in the time domain," *Transactions of the IRE Professional Group on Circuit Theory*, vol. 1, no. 3, pp. 29–39, 1954.

[4] M. Strieby, "A fourier method for time domain synthesis," in *Proc. of Symposium on Modern Network Theory, Polytechnic Inst. of Brooklyn*, pp. 197–209, 1955.

[5] A. Papoulis, "Network response in terms of behavior at imaginary frequencies," in *Proc. Symp. on Modern Network Synthesis*, vol. 5, p. 403, 1955.

[6] W. Huggins, "Signal theory," *IRE Transactions on Circuit Theory*, vol. 3, no. 4, pp. 210–216, 1956.

[7] E. G. Gilbert, "Linear system approximation by differential analyzer simulation of orthonormal approximation functions," *IRE Transactions on Electronic Computers*, no. 2, pp. 204–209, 1959.

[8] E. G. Gilbert and J. Otterman, "The synthesis of linear filters with real or imaginary transfer functions," *Transactions of the American Institute of Electrical Engineers, Part I: Communication and Electronics*, vol. 79, no. 3, pp. 323–330, 1960.

[9] N. Chakraborti, "The generation of pulse-like functions by means of lumped equivalents of delay lines," *Proceedings of the IEE-Part C: Monographs*, vol. 109, no. 15, pp. 117–125, 1962.

[10] B. Liu, "A time domain approximation method and its application to lumped delay lines," *IRE Transactions on Circuit Theory*, vol. 9, no. 3, pp. 256–261, 1962.

[11] F. Hli, "A general method for time domain network synthesis," *Transactions of the IRE Professional Group on Circuit Theory*, vol. 1, no. 3, pp. 21–28, 1954.

[12] R. A. Pucel, "Network synthesis for a prescribed impulse response using a real-part approximation," *Journal of Applied Physics*, vol. 28, no. 1, pp. 124–129, 1957.

[13] E. A. Guillemin, "Synthesis of passive networks: theory and methods appropriate to the realization and approximation problems," 1957.

[14] W. Yengst, "Approximation to a specified time response," *IRE Transactions on Circuit Theory*, vol. 9, no. 2, pp. 152–162, 1962.

[15] C. Vasiliu, "A practical method for time-domain network synthesis," *IEEE Transactions on Circuit Theory*, vol. 12, no. 2, pp. 234–241, 1965.

[16] E. Guillemin, "A historical account of the development of a design procedure for pulse forming networks," *NRDC Radiation Laboratory Report*, vol. 43, 1944.

[17] D. F. Tuttle, *Network synthesis for prescribed transient response*. PhD thesis, Massachusetts Institute of Technology. Department of Electrical Engineering, 1948.

[18] M. V. Cerrillo and E. A. Guillemin, *On Basic Existence Theorems: III. Theoretical Considerations on Rational Fraction Expansions for Network Functions*. Research Laboratory of Electronics, Massachusetts Institute of Technology, 1952.

[19] W. H. Kautz, "Network synthesis for specified transient response," 1952.

[20] B. Hli *et al.*, "Network synthesis by impulse response for specified input and output in the time domain," 1953.

[21] R. W. Hamming, *Digital filters*. Courier Corporation, 1989.

[22] S. A. Haddad, S. Bagga, and W. A. Serdijn, "Log-domain wavelet bases," *IEEE Transactions on Circuits and Systems I: Regular Papers*, vol. 52, no. 10, pp. 2023–2032, 2005.

[23] A. J. Casson and E. Rodriguez-Villegas, "A 60 pw g_mc continuous wavelet transform circuit for portable EEG systems," *IEEE Journal of Solid-State Circuits*, vol. 46, no. 6, pp. 1406–1415, 2011.

[24] A. Ljutic, S. Djukic, and M. Vucic, "Time-domain synthesis of linear-phase selective filters," in *MIPRO, 2010 Proceedings of the 33rd International Convention*, pp. 165–170, May 2010.

[25] M. Vucic and G. Molnar, "Time-domain synthesis of continuous-time systems based on second-order cone programming," *IEEE Transactions on Circuits and Systems I: Regular Papers*, vol. 55, pp. 3110–3118, Nov 2008.

[26] M. Vucic, G. Molnar, and S. Djukic, "Synthesis of linear-phase selective filters based on maximum of time-domain response," in *Circuits and Systems (ISCAS), 2011 IEEE International Symposium on*, pp. 1648–1651, May 2011.

[27] I. Filanovsky and P. Matkhanov, "Synthesis of time delay networks approximating the pulse response described by an integer power of a sinusoid over its semi-period," *Analog Integrated Circuits and Signal Processing*, vol. 28, no. 1, pp. 83–90, 2001.

[28] I. M. Filanovsky and P. N. Matkhanov, "Synthesis of a pulse-forming reactance network shaping a quasi-rectangular delayed output pulse," *IEEE Transactions on Circuits and Systems II: Express Briefs*, vol. 51, pp. 190–194, April 2004.

[29] I. M. Filanovsky and P. N. Matkhanov, "Synthesis of reactance networks shaping a quasi-rectangular pulse," *IEEE Transactions on Circuits and Systems II: Express Briefs*, vol. 52, pp. 242–245, May 2005.

[30] I. Daubechies *et al.*, *Ten lectures on wavelets*, vol. 61. SIAM, 1992.

[31] S. Mallat, *A wavelet tour of signal processing: the sparse way*. Academic press, 2008.

[32] O. Rioul and M. Vetterli, "Wavelets and signal processing," *IEEE signal processing magazine*, vol. 8, no. LCAV-ARTICLE-1991-005, pp. 14–38, 1991.

[33] S. A. Haddad, J. M. Karel, R. Peelers, R. L. Westra, W. Serdijn, *et al.*, "Ultra low-power analog morlet wavelet filter in 0.18 μm bicmos technology," in *Proceedings of the 31st European Solid-State Circuits Conference, 2005. ESSCIRC 2005.*, pp. 323–326, IEEE, 2005.

[34] P. R. Agostinho, S. A. Haddad, J. A. De Lima, and W. A. Serdijn, "An ultra low power CMOS pa/v transconductor and its application to wavelet filters," *Analog Integrated Circuits and Signal Processing*, vol. 57, no. 1-2, pp. 19–27, 2008.

[35] A. J. Casson and E. R. Villegas, "An inverse filter realisation of a single scale inverse continuous wavelet transform," in *IEEE International Symposium on Circuits and Systems, 2008. ISCAS 2008.*, pp. 904–907, IEEE, 2008.

[36] M. Tuckwell and C. Papavassiliou, "An analog Gabor transform using sub-threshold 180-nm CMOS devices," *IEEE Transactions on Circuits and Systems I: Regular Papers*, vol. 56, no. 12, pp. 2597–2608, 2009.

[37] J. M. H. Karel, *A wavelet approach to cardiac signal processing for low-power hardware applications*. Universitaire Pers Maastricht, 2009.

[38] M. Vucic and G. Molnar, "Measure for phase linearity based on symmetry of time-domain response," *Electron. Lett*, vol. 39, no. 19, pp. 1425–1426, 2003.

[39] M. Vucic and G. Molnar, "Equaliser design based on maximum of response to sinc pulse," *Electronics letters*, vol. 41, no. 19, pp. 1089–1090, 2005.

[40] J. Karel, R. Peeters, R. Westra, S. Haddad, and W. Serdijn, "An L2-based approach for wavelet approximation," in *Decision and Control, 2005 and 2005 European Control Conference. CDC-ECC'05. 44th IEEE Conference on*, pp. 7882–7887, IEEE, 2005.

[41] Y. Tong, Y. He, H. Li, W. Yu, and Y. Long, "Analog implementation of wavelet transform in switched-current circuits with high approximation precision and minimum circuit coefficients," *Circuits, Systems, and Signal Processing*, vol. 33, no. 8, pp. 2333–2361, 2014.

[42] M. Li and Y. He, "Analog wavelet transform using multiple-loop feedback switched-current filters and simulated annealing algorithms," *AEU-International Journal of Electronics and Communications*, vol. 68, no. 5, pp. 388–394, 2014.

[43] H. Li, Y. He, and Y. Sun, "A pso method for wavelet approximation," *Information Technology Journal*, vol. 13, no. 4, p. 661, 2014.

[44] H. Li, Y. He, and Y. Sun, "Optimal analog wavelet bases construction using hybrid optimization algorithm," *International Journal on Smart Sensing and Intelligent Systems*, vol. 9, no. 4, pp. 1918–1942, 2016.

[45] G. A. Baker and P. R. Graves-Morris, *Padé approximants*, vol. 59. Cambridge University Press, 1996.

[46] A. J. Casson, D. C. Yates, S. Patel, and E. Rodriguez-Villegas, "An analogue bandpass filter realisation of the continuous wavelet transform," in *Engineering in Medicine and Biology Society, 2007. EMBS 2007. 29th Annual International Conference of the IEEE*, pp. 1850–1854, IEEE, 2007.

[47] E. J. Weniger, "Nonlinear sequence transformations for the acceleration of convergence and the summation of divergent series," *Computer Physics Reports*, vol. 10, no. 5, pp. 189–371, 1989.

[48] A. Sidi, *Practical extrapolation methods: Theory and applications*, vol. 10. Cambridge University Press, 2003.

[49] C. Brezinski and M. R. Zaglia, *Extrapolation methods: theory and practice*, vol. 2. Elsevier, 2013.

[50] C. Brezinski, *Padé-type approximation and general orthogonal polynomials*. Springer, 1980.

[51] J. Wimp, *Sequence transformations and their applications*. Elsevier, 1981.

[52] G. I. Marchuk and V. V. Shaidurov, *Difference methods and their extrapolations*, vol. 19. Springer Science & Business Media, 2012.

[53] J.-P. Delahaye, *Sequence transformations*, vol. 11. Springer Science & Business Media, 2012.

[54] C. B. Liem, T. Shih, and T. Lü, *The splitting extrapolation method: a new technique in numerical solution of multidimensional problems*, vol. 7. World Scientific, 1995.

[55] A. Gil, J. Segura, and N. M. Temme, *Numerical methods for special functions*. SIAM, 2007.

[56] W. H. Press, *Numerical recipes 3rd edition: The art of scientific computing*. Cambridge university press, 2007.

[57] F. Bornemann, D. Laurie, S. Wagon, and J. Waldvogel, "The SIAM 100-digit challenge: A Study in high-accuracy numerical computing," *Society for Industrial Applied Mathematics*, 2004.

[58] K. Knopp, *Theory and application of infinite series*. Courier Corporation, 2013.

[59] D. Levin, "Development of non-linear transformations for improving convergence of sequences," *International Journal of Computer Mathematics*, vol. 3, no. 1-4, pp. 371–388, 1973.

[60] H. Xu, S. Jain, J. Song, T. Kamgaing, and Y. S. Mekonnen, "Acceleration of spectral domain immitance approach for generalized multilayered shielded microstrips using the Levin's transformation," *IEEE Antennas and Wireless Propagation Letters*, vol. 14, pp. 92–95, 2015.

[61] H. Xu, K. Chen, J. Song, T. Kamgaing, and Y. S. Mekonnen, "A novel approach to accelerate spectral domain approach for shielded microstrip lines using the levin transformations and summation-by-parts," *Radio Science*, vol. 49, no. 8, pp. 573–582, 2014.

[62] K. Sainath, F. L. Teixeira, and B. Donderici, "Complex-plane generalization of scalar levin transforms: A robust, rapidly convergent method to compute potentials and fields in multi-layered media," *Journal of Computational Physics*, vol. 269, pp. 403–422, 2014.

[63] H. Xu, J. Song, T. Kamgaing, and Y. Mekonnen, "The extrapolation methods in acceleration of sda for shielded microstrip lines," in *Antennas and Propagation Society International Symposium (APSURSI), 2014 IEEE*, pp. 2118–2119, IEEE, 2014.

[64] K. Sainath, F. Teixeira, and B. Donderici, "Complex-valued levin transforms: A robust algorithm for field computation in anisotropic-layered media," in *Antennas and Propagation Society International Symposium (APSURSI), 2014 IEEE*, pp. 2024–2025, IEEE, 2014.

[65] H. S. Xu, J. Da Zhu, and P. Dai, "Novel acceleration methods for electromagnetic modeling of high-speed interconnects in distribution grids asic," in *Electricity Distribution (CICED), 2016 China International Conference on*, pp. 1–5, IEEE, 2016.

[66] N. Krishnapura, S. Pavan, C. Mathiazhagan, and B. Ramamurthi, "A baseband pulse shaping filter for gaussian minimum shift keying," in *Circuits and Systems, 1998. ISCAS'98. Proceedings of the 1998 IEEE International Symposium on*, vol. 1, pp. 249–252, IEEE, 1998.

[67] S. M. Kashmiri, S. A. Haddad, and W. A. Serdijn, "High-performance analog delays: surpassing bessel-thomson by pade-approximated gaussians," in *Circuits and Systems, 2006. ISCAS 2006. Proceedings. 2006 IEEE International Symposium on*, pp. 4–pp, IEEE, 2006.

[68] A. J. Casson and E. Rodriguez-Villegas, "Nanowatt multi-scale continuous wavelet transform chip," *Electronics Letters*, vol. 50, no. 3, pp. 153–154, 2014.

[69] A. J. Casson, "An analog circuit approximation of the discrete wavelet transform for ultra low power signal processing in wearable sensor nodes," *Sensors*, vol. 15, no. 12, pp. 31914–31929, 2015.

[70] Y.-J. Min, H.-K. Kim, Y.-R. Kang, G.-S. Kim, J. Park, and S.-W. Kim, "Design of wavelet-based ECG detector for implantable cardiac pacemakers," *IEEE transactions on biomedical circuits and systems*, vol. 7, no. 4, pp. 426–436, 2013.

[71] J. Karel, R. Peeters, R. Westra, S. Haddad, and W. Serdijn, "Wavelet approximation for implementation in dynamic translinear circuits," in *Proc. 16th IFAC World Congress (IFAC WC'05), Prague, Czech republic, July 3*, vol. 8, 2005.

[72] J. Karel, R. Peeters, R. Westra, S. Haddad, and W. Serdijn, "An l 2-based approach for wavelet approximation," in *Decision and Control, 2005 and 2005 European Control Conference. CDC-ECC'05. 44th IEEE Conference on*, pp. 7882–7887, IEEE, 2005.

[73] H. Kamada and N. Aoshima, "Analog Gabor transform filter with complex first order system," in *SICE'97. Proceedings of the 36th SICE Annual Conference. International Session Papers*, pp. 925–930, IEEE, 1997.

[74] S. A. Haddad, W. Serdijn, *et al.*, "Mapping the wavelet transform onto silicon: the dynamic translinear approach," in *IEEE International Symposium on Circuits and Systems, 2002. ISCAS 2002.*, vol. 5, pp. V–621, IEEE, 2002.

[75] S. A. Haddad, R. Houben, W. Serdijn, *et al.*, "Analog wavelet transform employing dynamic translinear circuits for cardiac signal characterization," in *IEEE International Symposium on Circuits and Systems, 2003. ISCAS 2003.*, vol. 1, pp. I–121, IEEE, 2003.

[76] S. A. Haddad, N. Verwaal, R. Houben, W. Serdijn, *et al.*, "Optimized dynamic translinear implementation of the gaussian wavelet transform," in *IEEE International Symposium on Circuits and Systems, 2004. ISCAS 2004.*, vol. 1, pp. I–145, IEEE, 2004.

[77] S. A. Haddad, J. M. Karel, R. L. Peeters, R. L. Westra, W. Serdijn, *et al.*, "Analog complex wavelet filters," in *IEEE International Symposium on Circuits and Systems, 2005. ISCAS 2005.*, pp. 3287–3290, IEEE, 2005.

[78] K. Ogata and Y. Yang, "Modern control engineering," 1970.

[79] E. J. Weniger, "Irregular input data in convergence acceleration and summation processes: General considerations and some special gaussian hypergeometric series as model problems," *Computer physics communications*, vol. 133, no. 2, pp. 202–228, 2001.

[80] C. K. Chui and J.-z. Wang, "A cardinal spline approach to wavelets," *Proceedings of the American Mathematical Society*, vol. 113, no. 3, pp. 785–793, 1991.

[81] M. A. Unser, "Ten good reasons for using spline wavelets," in *Optical Science, Engineering and Instrumentation'97*, pp. 422–431, International Society for Optics and Photonics, 1997.

[82] M. Unser and T. Blu, "Cardinal exponential splines: part i-theory and filtering algorithms," *IEEE Transactions on Signal Processing*, vol. 53, no. 4, pp. 1425–1438, 2005.

[83] E. J. Weniger, "Mathematical properties of a new levin-type sequence transformation introduced by cizek, zamastil, and skála. i. algebraic theory," *Journal of mathematical physics*, vol. 45, no. 3, pp. 1209–1246, 2004.

[84] S. A. P. Haddad and W. A. Serdijn, *Ultra low-power biomedical signal processing: an analog wavelet filter approach for pacemakers*. Springer Science & Business Media, 2009.

[85] L. Pernebo and L. M. Silverman, "Model reduction via balanced state space representations," *Automatic Control, IEEE Transactions on*, vol. 27, no. 2, pp. 382–387, 1982.

[86] J. P. Marmorat and M. Olivi, "RARL2: a Matlab based software for H^2 rational approximation," 2004.

[87] M. Fahmy and M. Sobhy, "Selective constant delay filters with chebyshev passband amplitude response," *International Journal of Circuit Theory and Applications*, vol. 8, no. 2, pp. 190–195, 1980.

[88] D. Rhodes and I. H. Zabalawi, "Design of selective linear-phase filters with equiripple amplitude characteristics," *Circuits and Systems, IEEE Transactions on*, vol. 25, no. 12, pp. 989–1000, 1978.

[89] H. Baher and M. O'Malley, "Generalized approximation techniques for selective linear-phase digital and nonreciprocal lumped filters," *Circuits and Systems, IEEE Transactions on*, vol. 33, no. 12, pp. 1159–1169, 1986.

[90] M. Hibino, Y. Ishizaki, and H. Watanabe, "Design of chebyshev filters with flat group-delay characteristics," *IEEE Transactions on circuit theory*, vol. 15, no. 4, pp. 316–325, 1968.

[91] H. Gutsche, "Approximation of transfer functions for filters with equalized group-delay characteristics," *Siemens Forschungs-und Entwicklungsberichte*, vol. 2, no. 5, pp. 288–292, 1973.

[92] B. Rakovich and V. Litovski, "Least-squares monotonic lowpass filters with sharp cutoff," *Electronics Letters*, vol. 9, no. 4, pp. 75–76, 1973.

[93] B. Rakovich and V. Litovski, "Monotonic passband low-pass filters with chebyshev stopband attenuation," *IEEE Transactions on Acoustics, Speech, and Signal Processing*, vol. 22, no. 1, pp. 39–44, 1974.

[94] V. Litovski, "Synthesis of monotonic passband sharp cutoff filters with constant group delay response," *IEEE Transactions on Circuits and Systems*, vol. 26, no. 8, pp. 597–602, 1979.

[95] B. Rakovich, M. D. Radmanović, and M. Popovich, "Transfer functions of selective filters with equalised passband group delay response," in *IEE Proceedings G (Electronic Circuits and Systems)*, vol. 129, pp. 11–18, IET, 1982.

[96] S. Sadughi and H. Kim, "An approximation procedure for selective linear phase filters," *Circuits and Systems, IEEE Transactions on*, vol. 34, no. 8, pp. 967–969, 1987.

[97] S. Sadughi, G. Martens, and H. Kim, "Selective linear-phase filters with controllable amplitude response," *IEEE transactions on circuits and systems*, vol. 32, no. 8, pp. 858–862, 1985.

[98] D. Carvalho, R. Seara, *et al.*, "Impulse response symmetry error for designing phase equalisers," *Electronics Letters*, vol. 35, no. 13, pp. 1052–1054, 1999.

[99] X. Huang, S. Jing, Z. Wang, Y. Xu, and Y. Zheng, "Closed-form fir filter design based on convolution window spectrum interpolation," *IEEE Transactions on Signal Processing*, vol. 64, pp. 1173–1186, March 2016.

[100] J.-H. Ahlberg, E.-N. Nilson, and J.-L. Walsh, "The theory of splines and their applications," 1968.

[101] M. Unser and T. Blu, "Fractional splines and wavelets," *SIAM review*, vol. 42, no. 1, pp. 43–67, 2000.

[102] T. Deliyannis, Y. Sun, and J. K. Fidler, *Continuous-time active filter design*. Crc Press, 1998.

[103] Y. Sun and J. K. Fidler, "Synthesis and performance analysis of universal minimum component integrator-based iflf ota-grounded capacitor filter," *Circuits, Devices and Systems, IEE Proceedings* -, vol. 143, pp. 107–114, Apr 1996.

[104] B. Linares-Barranco and T. Serrano-Gotarredona, "On the design and characterization of femtoampere current-mode circuits," *Solid-State Circuits, IEEE Journal of*, vol. 38, no. 8, pp. 1353–1363, 2003.

[105] A. Veeravalli, E. Sanchez-Sinencio, and J. Silva-Martinez, "Different operational transconductance amplifier topologies for obtaining very small transconductances," in *Circuits and Systems, 2000. Proceedings. ISCAS 2000 Geneva. The 2000 IEEE International Symposium on*, vol. 4, pp. 189–192, IEEE, 2000.

Publications Related to this Thesis

[1] G. Makkena and M. B. Srinivas, "Nonlinear sequence transformation-based continuous-time wavelet filter approximation," *Circuits, Systems, and Signal Processing*, Springer- Online First, June 14 2017 pp. 1–19.

[2] G. Makkena and M. B. Srinivas, "Closed-Form Design of Continuous-Time Linear-Phase Selective Filters," *IEEE Signal Processing Letters*,(communicated).

[3] G. Makkena, K. Abhilash, and M. B. Srinivas, "Gaussian filter approximation using Levin's transformation for implementation in analog domain," in *IEEE Asia Pacific Conference on Postgraduate Research in Microelectronics and Electronics, IEEE PrimeAsia, 2013*, pp. 204–207, IEEE, 2013.

[4] G. Makkena, P. R. Bvvsn, and M. B. Srinivas, "Uniform approximation of gaussian wavelet for biomedical signal processing in analog domain," in *Engineering in Medicine and Biology Society (EMBC), 2013 35th Annual International Conference of the IEEE*, pp. 2886–2889, IEEE, 2013.

Other Publications

[1] C. Vudadha, G. Makkena, M. V. S. Nayudu, P. S. Phaneendra, S. E. Ahmed, S. Veeramachaneni, N. M. Muthukrishnan, and M. B. Srinivas, "Low-power self reconfigurable multiplexer based decoder for adaptive resolution flash adcs," in *VLSI Design (VLSID), 2012 25th International Conference on*, pp. 280–285, IEEE, 2012.

[2] C. Vudadha, P. S. Phaneendra, G. Makkena, V. Sreehari, N. M. Muthukrishnan, and M. B. Srinivas, "Design of cnfet based ternary comparator using grouping logic," in *Faible Tension Faible Consommation (FTFC), 2012 IEEE*, pp. 1–4, IEEE, 2012.

[3] A. S. Vaidya, G. Makkena, V. Srihari, M. B. Srinivas, and S. K. Rao, "A sustainable solution for monitoring malnutrition in children in developing countries," in *Global Humanitarian Technology Conference: South Asia Satellite (GHTC-SAS), 2013 IEEE*, pp. 170–174, IEEE, 2013.

Biography of the Candidate

Goutham Makkena obtained his Masters in Microelectronics from Birla Institute of Technology and Science - Pilani, Hyderabad Campus and is currently pursuing Ph.D in the Electrical Engineering department of the same University. His research interests include continuous-time filter approximation, time-domain synthesis and low power mixed signal IC design.

Biography of the Supervisor

Prof. M. B. Srinivas is presently Dean, School of Engineering and Technology at B. M. L. Munjal University, Gurgaon, India. He was earlier a Professor of Electrical Engineering at Birla Institute of Technology and Science (BITS)-Pilani, Hyderabad Campus, India, from where he is currently on leave. He obtained his Ph.D. degree from Indian Institute of Science (IISc), Bangalore in 1991. His research interests include high performance logic design, VLSI arithmetic, data converters and reversible computing.